nature reviews physics

https://doi.org/10.1038/s42254-023-00617-9

Technical review

Check for updates

The role of particle shape in computational modelling of granular matter

Jidong Zhao [1] ✉, Shiwei Zhao [1] ✉ & Stefan Luding [2]

Abstract

Granular matter is ubiquitous in nature and is present in diverse forms in important engineering, industrial and natural processes. Particle-based computational modelling has become indispensable to understand and predict the complex behaviour of granular matter in these processes. The success of modern computational models requires realistic and efficient consideration of particle shape. Realistic particle shapes in naturally occurring and engineered materials offer diverse challenges owing to their multiscale nature in both length and time. Furthermore, the complex interactions with other materials, such as interstitial fluids, are highly nonlinear and commonly involve multiphysics coupling. This Technical Review presents a comprehensive appraisal of state-of-the-art computational models for granular particles of either naturally occurring shapes or engineered geometries. It focuses on particle shape characterization, representation and implementation, as well as its important effects. In addition, the particles may be hard, highly deformable, crushable or phase transformable; they might change their behaviour in the presence of interstitial fluids and are sensitive to density, confining stress and flow state. We describe generic methodologies that capture the universal features of granular matter and some unique approaches developed for special but important applications.

Sections

[1]The Hong Kong University of Science and Technology, Hong Kong, China. [2]The University of Twente, Enschede, The Netherlands. ✉e-mail: jzhao@ust.hk; ceswzhao@ust.hk

Key points

- Particle-based computational modelling that considers realistic particle shapes has become indispensable for understanding and predicting the complex behaviour of granular matter in engineering, industry and nature.
- How to effectively represent the shape of a particle is closely related to its intended purpose; the modelling of naturally occurring granular materials may differ from approaches for engineered particles.
- Particle shape representation is inseparably coupled to the detection of interparticle contacts, both of which critically determine the computational accuracy and efficiency of simulations of granular matter.
- Specific methodologies are needed to address challenges arising from crushable particles or highly deformable particles, in which the co-evolution of particle shapes and sizes and hence contact detection algorithms dictate both accuracy and efficiency.
- Consideration of shape effects in coupled simulations of granular particles and environmental fluids requires revamped theories and methods to faithfully reflect their underpinning multiphase, multiphysics nature.
- Incorporating realistic particle shapes in granular matter modelling must harness the latest advances in parallel computing and machine learning for effective large-scale computations.

Introduction

Granular media are ubiquitous in nature and indispensable in everyday life. Broadly speaking, granular matter may include both densely packed solid, macroscopic particles interacting through dissipative processes and microparticle to nanoparticle in suspension. They are present in diverse forms spanning nanoscale, engineering and even planetary scales. Examples of the particles forming granular media include biological viruses[1], colloids[2], nanoparticles[3], red blood cells[4], microplastics[5], beach sand[6], food grains[7], chemical powders[8], boulders[9], icebergs[10] and asteroids[11]. Granular media exhibit emergent phenomena at various length scales and timescales, including jamming, collapse, failure, avalanche, phase transition and flow. These complex behaviours are underpinned by interactions between particles and between particles and their environment; the shape of a particle has a crucial role in such interactions. The past decades have witnessed a rapid development of computational models and numerical methods that foster better models and thus improved predictions and deeper understanding. Although conventional approaches based on simplified particle shapes such as spheres have gained great success in various scientific and engineering fields, recent research has paid more attention to the high-resolution representation and accurate modelling of particle shapes. Indeed, particle shape can be intricately intertwined with many facets of granular behaviour. For example, granular matter consisting of crushable and/or deformable particles involves evolving particle shapes and is notably different from hard-particle systems. Frequently, granular matter exists in a multiphysics environment in which particle shape critically affects key processes such as particle–fluid interaction. This Technical Review aims to make a critical comparison of state-of-the-art computational models and numerical techniques for granular matter (Fig. 1) prevailing in recent years for modelling realistic particle shapes and to offer perspectives for emerging challenges.

We organize the Technical Review according to the following subtopics. We first discuss numerical models of hard granular particles with arbitrary shapes and that are rigid and unbreakable and in the absence of multiphysics fields, with focus on computational models of contact interactions between particles. We then turn to the characterization and simulation of crushable and/or deformable particles with intermittent or continuous changes in particle shape that may be strongly coupled to the mechanical responses of an assembly. Next, we discuss modelling granular particles in multiphysics fields highlighting the complications caused by particle–fluid interactions. We then discuss advanced numerical techniques, which use direct numerical simulation (DNS) approaches, parallel computing or machine learning (ML) and which enable and accelerate large-scale, multiscale simulations of granular matter. Finally, we describe some future challenges for the computational modelling of granular matter.

Hard granular particles

Shape matters

Naturally occurring granular matter. Granular matter in nature exists in diverse shapes across different scales in both size and time (Fig. 1). The shapes of food grains, such as maize, wheat and coffee beans[7,12], critically affect their flow, packing and processing including mixing and grinding. Naturally occurring sand grains are typically non-spherical because of their mineral composition and geohydrochemical environments and history. The effect of their shape is manifest in various facets of their engineering properties, including shear strength, flow behaviour (such as hopper discharge in silo or reactor core[13]), wave propagation[14], segregation[15] and cohesive powder flow[8]. The collective behaviour of biorelated granular media, including biomass particles[16,17] and creatures such as sea stars, is well known to depend strongly on their particle shape; the same is true of asteroids[11,18]. Human activities engender the generation and accumulation of microparticles in the natural environment, including nanoplastics and microplastics[5] and atmospheric particulate matter[19], threatening the safety of our lives. Representative examples of modelling techniques used to study granular materials in the natural world are the discrete element method (DEM) for studies on particle scales and molecular dynamics (MD) for studies on atomistic scales.

Granular matter by design. Unlike naturally occurring particles, granular materials can be purposely designed or engineered to have desired functions and macroscopic properties. Numerical modelling is effective at the design stage. For example, with precisely controlled geometry, non-convex interlocking granular particles may be programmed to form structured fabrics that offer desirable mechanical properties of jamming and unjamming transitions that are useful in medical or engineering applications[20,21]. An example application is aleatory architecture[21]. DEM has been widely used for aggregations of such designed-shape particles to achieve tunable mechanical properties[20] and to serve in applications including architectural construction[22]. The design and testing of specially shaped nanoparticles and colloidal particles have become an emerging technology for creating functional nanostructures[23,24] or smart materials via processes such as reversible assembly[25] and magnetic assembly[26]. On this scale, MD[27,28] is prevalent as a simulation tool. Particle shape has an underpinning role for inactive

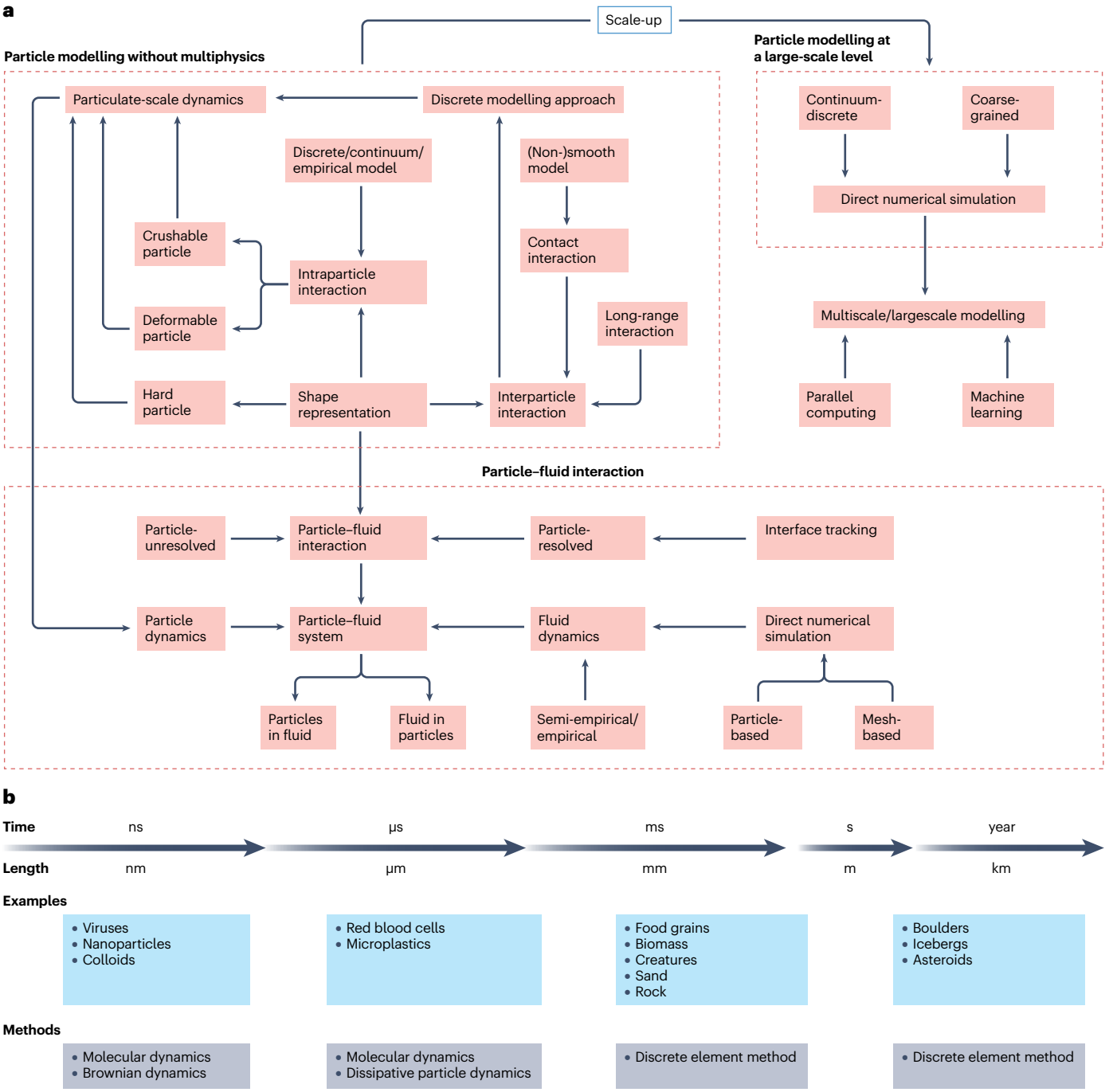

Fig. 1 | Modelling realistic complex particles and their collective behaviours. a, Relationship between different methods and systems. **b**, Shape matters in granular matter across multiple scales.

nanoparticles and microparticles that are ultrasound-propelled[3,29] or driven by active particle aggregations[30] and self-assembling structures of colloidal particles[2]. Such systems have been treated numerically using Brownian dynamics[31,32], dissipative particle dynamics (DPD)[33], Monte Carlo (MC)[34] and MD[35]. Moreover, particle shape is of major concern in the design of energy cells because aspherical-active particles can cause non-uniform lithium intercalation[36] in Li-ion batteries.

Shape representation

Qualitative or quantitative terminologies such as convexity, regularity, symmetry, sphericity, elongation and flatness have been used to describe particle shapes. Naturally occurring particles commonly have arbitrary (concave and irregular) shapes, whereas regular shapes that are easy to describe, manipulate and manufacture are often preferred in designed granular matter. We summarize three major schemes

a Primitive clumped scheme

Sphere-clump method

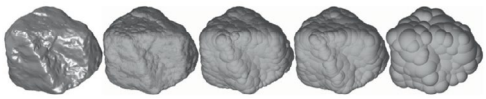

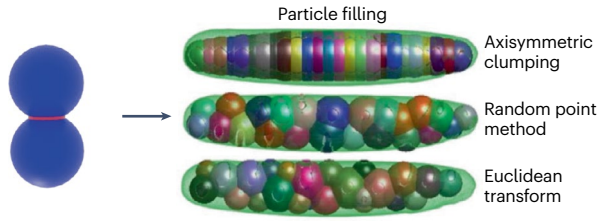

Sphere-cluster method

b Mesh-based scheme

Triangular meshes

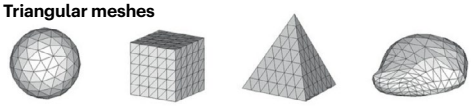

Nodes based on the meshes

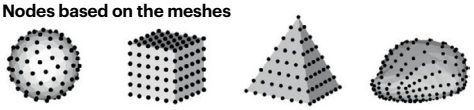

Tetrapods

Spherotetrahedron

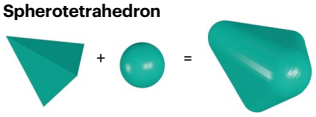

Cubic supercells

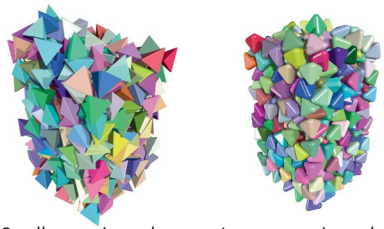

Small sweeping sphere Large sweeping sphere

c Analytical-surface scheme

Superellipsoid

$$\left(\left| \frac{x}{r_x} \right|^{\frac{2}{\varepsilon_1}} + \left| \frac{y}{r_y} \right|^{\frac{2}{\varepsilon_1}} \right)^{\frac{\varepsilon_1}{\varepsilon_2}} + \left| \frac{z}{r_z} \right|^{\frac{2}{\varepsilon_2}} = 1$$

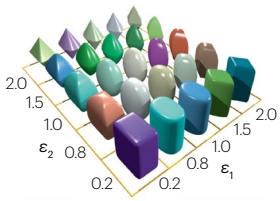

Poly-superellipsoid

$$\left(\left| \frac{x}{r_{xi}} \right|^{\frac{2}{\varepsilon_{1i}}} + \left| \frac{y}{r_{yi}} \right|^{\frac{2}{\varepsilon_{1i}}} \right)^{\frac{\varepsilon_{1i}}{\varepsilon_{2i}}} + \left| \frac{z}{r_{zi}} \right|^{\frac{2}{\varepsilon_{2i}}} = 1$$

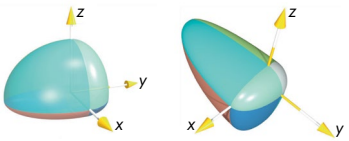

NURBS

$$\boldsymbol{S}(u,v) = \frac{\sum_{i=0}^{n} \sum_{j=0}^{m} N_{i,p}(u) N_{j,q}(v) W_{i,j} \boldsymbol{p}_{i,j}}{\sum_{i=0}^{n} \sum_{j=0}^{m} N_{i,p}(u) N_{j,q}(v) W_{i,j}}$$

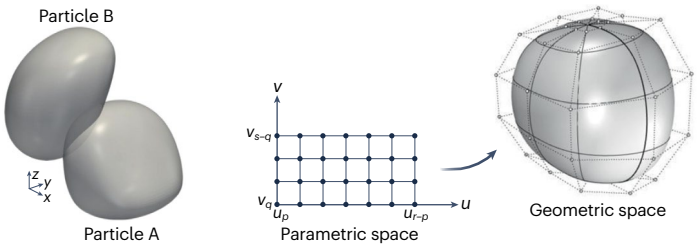

Fourier spectrum

$$r_i(\theta_i) = r_0 + \sum_{n=1}^{N} [A_n \cos(n\theta) + B_n \sin(n\theta)]$$

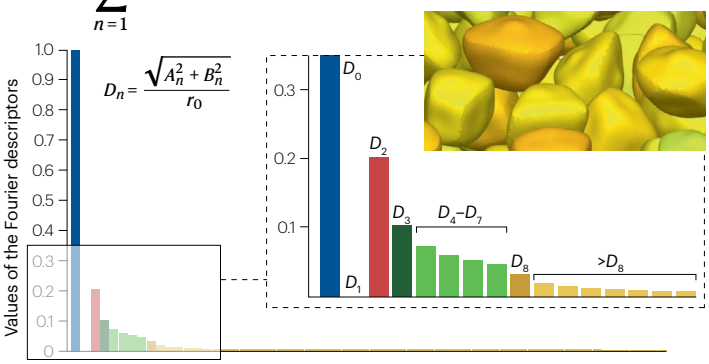

Spherical harmonics

$$\boldsymbol{r}(\theta,\varphi) = \sum_{n=0}^{N} \sum_{m=-n}^{n} \left(\alpha_n^m \sqrt{\frac{(2n+1)(n-|m|)!}{4\pi(n+|m|)!}} \boldsymbol{P}_n^m(\cos\theta) e^{im\varphi} \right)$$

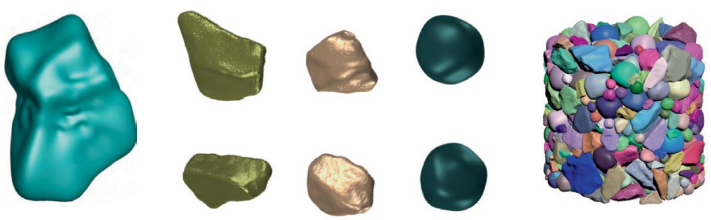

Fig. 2 | Numerical models on particle shape representation. a, Primitive-clumped scheme. The sphere-clump and sphere-cluster methods are exemplified here. The sphere-clump method allows overlaps but needs proper consideration of moment of inertia for rotational modelling. Showcased are different particle filling methods with varying efficiencies and accuracies. The sphere-cluster method does not allow overlaps and needs more spheres to fill a particle. **b**, A mesh-based scheme uses vertices and polygons or polyhedrons and Minkowski sum of them to represent a particle. **c**, Analytical-surface scheme. Part **a** adapted with permission from ref. 202, Elsevier, and ref. 203, ICE Publishing. Part **b** adapted with permission from ref. 40, Springer, and ref. 94, Elsevier. Part **c** adapted with permission from the following: superellipsoid and poly-superellipsoid[50], Wiley; non-uniform rational B-spline (NURBS)[53], Elsevier; Fourier spectrum[55], Elsevier; and spherical harmonics (ref. 57, Springer, and ref. 84, Elsevier). For definitions of variables, see the corresponding references.

for representing shape in the computational modelling of granular matter (Fig. 2).

Primitive-clumped scheme. This scheme refers to a class of methods that approximate the complex shape of grains by aggregating a set of simple geometric primitives such as points, discs, spheres or cylinders. There are two prevailing approaches to aggregating primitives: one simply clumps the primitives together to obtain the best-fit shape profile by allowing arbitrary overlapping between the primitives, exemplified by such methods as sphere-clump particles[37] and cross-shaped particles[38]; the other is the so-called cluster approach in which the overlap between the primitives is constrained by taking interprimitive interactions into consideration. Typical methods in this category include the sphere-cluster particle and the point-cluster (cloud) particle[27]. The cluster-type particle methods often require many primitives to render sufficient representation of the realistic shape, which may incur increasing computational cost and hinder their application for modelling large-scale systems. As also noted in ref. 39, the clustered particle is often rougher than the original smooth shape to be approximated, which leads to increased friction and interlocking effects between clustered particles and hence undesirable physical behaviour in simulations.

Mesh-based scheme. In a typical mesh-based scheme, the shape of a grain is represented by a collection of vertices and polygons. The polygons may range from typical triangles to simple, convex and regular polyhedra such as platonic solids and irregular polyhedra[40]. The approximation of complex shapes in this scheme strongly depends on the resolution of vertices. To reduce the roughness of the mesh-based surface, the Minkowski-sum representation has become an increasingly popular and effective extension. In d dimensions, a sphere $\mathbf{R}$ is typically swept over a mesh-based surface $\mathbf{S}$ to obtain the Minkowski sum of the two, namely,

$$\mathbf{S} \oplus \mathbf{R} = \{s + r | s \in \mathbf{S}, r \in \mathbf{R}\}, \mathbf{S}, \mathbf{R} \in \mathbb{R}^d \quad (1)$$

For example, sweeping a sphere along a segment may yield a thick bar (spherocylinder[41]), along all edges (segments) of a polygon for a spheropolygon[42], or along the surface of a polyhedron for a dilated polyhedron[43] or generally called spheropolyhedron[44]. Notably, some mesh-based representations of particle shape cause a non-smoothness issue of the particle surface at vertices and edges, posing computational challenges. Rounding the vertices or edges by using arcs or spheres (that is, the Minkowski-sum method) to remove the non-smoothness issue is a possible remedy[39]. Moreover, the mesh-based scheme is the most flexible of the methods discussed here to represent arbitrarily shaped particles, and the vertices can be readily utilized as Lagrangian points to compute particle–fluid interactions (as discussed in the section on particle–fluid interactions). However, mesh-based schemes require sophisticated hierarchical data structures to store the topology of vertices, edges and facets.

Analytical-surface scheme. A shape can be represented analytically by a surface function. Although a sphere is the most straightforward example that exists in a wide family of ellipsoids and superellipsoids[45–47], analytical function-based poly-ellipsoids[48,49] and poly-superellipsoids[50] can provide more asymmetric features. Following the concept of clumping, combining different surface functions may offer other shape representations such as poly-Béziers[51] and meta-balls[52]. Although these analytical surfaces can be taken as primitives to construct complex shapes in the spirit of the primitive-clumped scheme, they may fail to model arbitrary, concave shapes directly. More advanced mathematical representations have been developed to obtain more flexible particle shapes. For example, non-uniform rational B-splines (NURBS) commonly used in computer graphics and computer-aided design have been used to represent particle shapes. A NURBS surface can be either convex[53] or concave[54], depending on the distribution of control points. This feature of NURBS may also be relevant to particle interaction, as discussed in the following section.

Fourier-spectrum-based representations offer another useful tool to generate three orthogonal cross-sections of a particle before interpolating them into a 3D surface[6,55]. As a further extension of Fourier-spectrum-based representation, spherical harmonics (SH) use higher-dimensional functions with linear combinations of Fourier series defined on a sphere to capture the morphology of realistic particles[56,57]. Both Fourier-spectrum-based and SH-based representations can be controlled by a given set of shape descriptors to generate virtual samples with shape characteristics statistically consistent with real samples. This feature is notably useful for generating a larger numerical sample from limited laboratory data. As a further extension of SH, harmonic functions can be also defined on an ellipsoid, in other words, ellipsoidal harmonics (EH). Although complicated in mathematical implementation, EH is a promising tool for representing non-spherical shapes because of the higher rate of numerical convergence[58]. Indeed, EH has been applied successfully to calculate the gravitational field of asteroids with complex shapes[59] and has proven to be superior to SH for highly elongated or concave shapes[60]. Note that the surface functions of Fourier-spectrum-based, SH and EH shapes are typically not used directly in the computation of inter-particle contact interactions. Instead, computational efficiency is improved by making further approximations using methods such as sphere clumping, clustering or mesh-based approaches.

Discrete modelling approaches

Discrete modelling approaches such as MD, MC and DEM (Table 1) have been applied widely in simulations of problems at scales including atomic, mesoscale, industrial and engineering, even to the astrophysical scale. It is common to assume that particle motion is governed by the Newton–Euler equations for time-driven dynamics:

$$m\frac{\mathrm{d}\mathbf{v}}{\mathrm{d}t} = \sum \mathbf{f}^{\mathrm{c}} + \mathbf{F}^{\mathrm{b}} \quad (2)$$

Table 1 | Computational modelling approaches for particle dynamics

Method	Description	Useful for	Limitations
Standard DEM (discrete element method)	Time driven Interparticle contact force is explicitly calculated with a given penetration–force contact model Particles are explicitly driven by the resolved contact force in conjunction with externally exerted forces	Allows smooth particle velocity solution Resolves contact forces easily Convenient to implement for non-spherical particles	Small time steps are required to ensure numerical stability Elaborated calibration of non-physical model parameters, including contact model parameters and damping, may be needed.
Contact dynamics	Time-driven or event-driven (but the event-driven may not be suitable for many-contact systems) No interparticle penetration allowed Solves a complementarity relation between contact velocity and impulse and indirectly solves the contact forces as a complementary to constraints	Implicit integrator allows large time step and good stability properties Contact forces are retrievable through impulse reaction if necessary Less artificial contact parameters as introduced in standard DEM Easy to handle particle shapes	Solving the complementarity problem is often time-consuming, especially for non-spherical particles Considerable oscillations may be introduced in retrieving contact forces Uniqueness of reactions not guaranteed
Impulse-based DEM (simultaneous)	Time-driven Particle motion is governed by Newton's law of impact Impulse applied in a simultaneous manner	Allows larger time step than standard DEM More computationally efficient than standard DEM Updating particle velocity by contact impulse	Can be as complicated as contact dynamics in implementation
Impulse-based DEM (sequential)	Time-driven Particle motion is governed by Newton's law of impact Impulse applied in a sequential manner	More computationally efficient than standard DEM Updating particle velocity by contact impulse Can be implemented straightforwardly	Results may depend on the handling order of contacts[68]
Event-driven DEM or molecular dynamics (MD)	Particle position updates with non-smooth velocities Simulation advances in collision event sequentially	Generally faster than standard DEM and MD	Limited to simple-shape particles and relatively dilute systems such as gas or suspended granular system Difficult in dealing with externally exerted forces such as gravitational, electrostatic or aerodynamic forces[201]
Monte Carlo method	Popularly used to simulate random jammed packing of non-spherical particles	Useful to model states of equilibrium	Requires a combination with other methods such as MD for dynamic problems
Brownian dynamics	No inertia force term involved but with additional stochastic body force Like DEM and MD, it can be either time-driven or event-driven	Replaces molecular interactions with stochastic forces and allows larger timescales than MD Useful to model complex fluids such as polymers and proteins in non-equilibrium situations	Limited to microscopic simulations such as colloidal liquid crystals and motion of bacteria
Material point method	Lagrangian material points moving on a Eulerian background mesh Material points interact with one another through the background nodes	Capable of solving large-deformation problems in both solid and fluid mechanics. Easy to deal with contacts between multimaterials	Requires complicated implementation for simulating material damage and fracture
Smoothed particle hydrodynamics	Uses a smooth kernel function for point-based integration at each Lagrangian point	Originally proposed for astrophysical problems, increasingly used in fluid mechanics and extended in solid mechanics	May not be suitable for high Reynolds number or turbulent flows Difficult to deal with fully incompressible fluids
Peridynamics	Uses integral of nonlocal forces to replace divergence of stress in the linear momentum equation A material point interacts with all neighbouring points within its horizon through pairwise bonds	Suitable for modelling fractures in solid without a pre-defined crack path Capable of modelling complex crack patterns such as branching and merging cracks	May not be suitable for simulating crack propagation in materials with high plastic deformation
Lattice Boltzmann method	Solves the lattice Boltzmann equation with imaginary fluid particles moving on the lattice grid	Easy to implement and highly suitable for parallel computing Suitable for simulating multiphase problems	Difficult to deal with high-Mach number flows Possible but less efficient to be extended to an unstructured grid
Dissipative particle dynamics (DPD)	Solves the stochastic differential equations of motion for particles involving conservative, dissipative and stochastic forces	Capable of modelling soft matter and complex fluids	Limited to mesoscale systems such as colloids, blood, polymers and so on Can be extended to consider multibody interactions (MDPD) and non-isothermal situations (EDPD)[169]
Lattice element method	Lattice-spring and lattice-beam modes are widely used for the interaction between lattice nodes The lattice grid can be structured or unstructured for forming regular or irregular lattice topologies, respectively	Easy to implement as cohesive DEM (with cohesive bonds at interparticle contacts) Useful for modelling crack propagation and failure in interparticle interfaces under quasi-static conditions	Requires a regular or irregular lattice structure, which may not be suitable for modelling irregular particle shapes Requires more implementation of contact interaction and detection for dynamic problems such as dynamic fragmentation

$$\mathbf{J}\frac{\mathrm{d}\boldsymbol{\omega}}{\mathrm{d}t}+\boldsymbol{\omega}\times(\mathbf{J}\boldsymbol{\omega})=\sum\mathbf{f}^{\mathrm{c}}\times\mathbf{r}^{\mathrm{c}} \quad (3)$$

in which m is the particle mass, $\mathbf{J}$ is the inertial moment, $\mathbf{v}$ is the translational velocity, $\boldsymbol{\omega}$ is the angular velocity, $\mathbf{f}^{\mathrm{c}}$ is the contact force, $\mathbf{r}^{\mathrm{c}}$ is the position vector of the contact point with respect to the mass centre and $\mathbf{F}^{\mathrm{b}}$ is the body force. The impulse-based versions of these equations are given as:

$$m\Delta\mathbf{v}=\sum\boldsymbol{\imath}^{\mathrm{c}}+\mathbf{F}^{\mathrm{b}}\Delta t \quad (4)$$

$$\mathbf{J}\Delta\boldsymbol{\omega}+\boldsymbol{\omega}\times(\mathbf{J}\boldsymbol{\omega})\Delta t=\sum\boldsymbol{\imath}^{\mathrm{c}}\times\mathbf{r}^{\mathrm{c}} \quad (5)$$

in which $\boldsymbol{\imath}^{\mathrm{c}}$ is the impulse at the contact and Δt is the time interval. To facilitate numerical implementation, a body-fixed frame is often applied, and quaternions are used to track particle rotation in equations (3) and (5).

DEM. As shown in Table 1, in addition to the standard form methods such as the standard 'soft-body' DEM[61], variants have been developed to suit specific purposes, including event-driven (ED) DEM[62], contact dynamics (CD)[63] and impulse-based DEM[64]. Standard DEM allows the possibility of particles interpenetrating, so that the interaction can be resolved by calculating the contact force explicitly using a given penetration–force contact model. Particle motion is resolved by explicitly solving equations (2) and (3) with integration schemes such as Verlet, velocity Verlet or predictor–corrector. ED tracks interparticle collision events by sorting the potential collision time for all pairs of particles in a simulation body, in which the particle velocity is updated from the restitution upon collision. Similar to ED, CD (or more accurately, non-smooth CD) also assumes impenetrable particles and requires the tracking of dynamic contacts in the system, as its name suggests. However, CD solves the velocity and the impulse at each contact for subsequent updates of the particle states. Although traditional ED has no static limit, CD is designed around static equilibrium, but neither works well for the opposite limit. DEM can tackle both. Unlike the standard DEM in which particle velocities and contact forces are solved smoothly, CD solves a complementarity relation between contact velocity and impulse and indirectly solves the contact forces as a complement to constraints (typically volume exclusion and non-sliding constraints for frictional granular systems), for example,

$$\mathbf{v}_{\mathrm{n}}^{\mathrm{c}}\geq 0,\ \mathbf{f}_{\mathrm{n}}^{\mathrm{c}}\geq 0,\ \mathbf{f}_{\mathrm{n}}^{\mathrm{c}}\cdot\mathbf{v}_{\mathrm{n}}^{\mathrm{c}}=0\ \text{(volume exclusion)} \quad (6)$$

$$\begin{cases}|\mathbf{v}_{\mathrm{t}}^{\mathrm{c}}|=0\Longrightarrow|\mathbf{f}_{\mathrm{t}}^{\mathrm{c}}|\leq\mu|\mathbf{f}_{\mathrm{n}}^{\mathrm{c}}|\\ |\mathbf{v}_{\mathrm{t}}^{\mathrm{c}}|\neq 0\Longrightarrow|\mathbf{f}_{\mathrm{t}}^{\mathrm{c}}|=\mu|\mathbf{f}_{\mathrm{n}}^{\mathrm{c}}|\end{cases}\text{(Coulomb law)} \quad (7)$$

in which μ is the coefficient of friction; $\mathbf{f}_{\mathrm{n}}^{\mathrm{c}}$ and $\mathbf{f}_{\mathrm{t}}^{\mathrm{c}}$ are normal and tangential contact forces, respectively; and $\mathbf{v}_{\mathrm{n}}^{\mathrm{c}}$ and $\mathbf{v}_{\mathrm{t}}^{\mathrm{c}}$ are normal and tangential relative contact velocities, respectively. Note that CD is more complex to implement than the standard DEM (as compared in refs. 65,66), which may limit its widespread use. Impulse-based DEM was originally proposed and widely used in computer graphics[67]. It applies Newton's law of impact, that is, equations (4) and (5), to determine the non-smooth particle velocity. Depending on the solution procedure, impulse-based DEM can be divided into two categories: the simultaneous impulse method and the sequential (or propagation) impulse method[68]. The simultaneous impulse method enforces constraints on all contacts at the same time and formulates a complementarity problem equivalent to the CD method[68]. The sequential impulse method applies the impulse to each contact one after another, a feature rendering it suitable for parallelization. Both methods have advantages and disadvantages[69]. Note that an iterative process is still required for the sequential method at each time step.

MD and MC. MD is very similar to DEM in its theoretical framework, and DEM can be considered a branch of MD. A noteworthy difference between MD and DEM is that MD is widely adopted to model atomic, molecular or nanoscale interactions between particles, for applications such as simulating Janus ring polymers[70]. Event-driven MD advances over time in terms of interparticle collision events. Only spherical particles have a closed form for collision prediction[62], and it is necessary to find the event time for non-spherical particles iteratively[71]. Similar to MD, Brownian dynamics (BD) can be used to simulate molecular-scale dynamics[72]. As a counterpart of the event-driven DEM or MD, MC has been used widely to model hard-body systems. It has applications in systems in static equilibrium[62], such as colloidal preassembly of superballs[73], the phase behaviour of hard curved spherocylinders[74] and the magnetic-field-assisted assembly of ellipsoids[75]. However, MC is generally unable to deal with the dynamics and time evolution of granular matter.

Interparticle contact interaction

Shape is an even more critical issue for interparticle interactions than for their geometric representation. This is especially true for contact interactions when modelling a granular assembly computationally. Contact interactions are commonly modelled by either smooth (force-based, 'soft-body') or non-smooth (impulse-based, 'hard-body') approaches[76] (Box 1). In either method, interparticle contacts or collisions must first be detected accurately and efficiently; doing so it poses a challenge when modelling non-spherical particles. Practical measures to balance the accuracy and efficiency of contact detection can be categorized into broad-phase and narrow-phase resolution techniques. The broad-phase methods aim to identify potential contacting pairs of particles by excluding most non-contacting pairs, whereas narrow-phase techniques offer an exact treatment of contact details such as the contact point, normal and tangential directions and contact penetration and/or deformation if any.

Broad-phase contact detection. Although linked cells are the standard method from MD for similarly sized spheres, the use of a bounding box, such as an axis-aligned bounding box, is a prevalent technique for broad-phase contact detection of non-spheres. Well-known algorithms include the sweep-and-prune algorithm, the cell-based algorithm and tree-based algorithms such as bounding volume hierarchy[77]. The sweep-and-prune algorithm is robust but not well suited for parallelization. The cell-based algorithm is known to be sensitive to the particle size distribution and must resort to remedies such as the stencil algorithm[78], which are complicated to implement. Polydispersity is efficiently accounted for by so-called hierarchical grid methods that stacks multiple scale-linked cells. Frequently, the cell-based methods must fill the entire simulation domain with cells, which demands high memory use and computational cost, especially for spatially sparse particles. The hierarchical grid uses either efficient binary search or tree-based algorithms to mitigate this issue. Such methods are widely used in computer graphics, for instance, in ray tracing and physics engines, and have been proven to be robust and efficient. An apparent

Box 1

Interparticle and intraparticle interactions

N-body problem

In an *N*-body problem, each individual particle in a system has non-contact interactions with the other particles. Such a model describes interasteroid gravitation and intermolecular van der Waals force, among others. Introducing a cut-off distance or tree data structures can reduce the time complexity substantially[76].

Smooth and non-smooth contact modelling

Smooth contact modelling allows interparticle penetration such that contact forces are calculated by a penalty-based law (see the figure, panel **a**, in which d_n^c, d_t^c are the normal penetration depth and tangential displacement, respectively; the other symbols are defined in equation (7) in the main text). Non-smooth contact modelling prohibits interparticle penetration such that contact force and velocity follow a complementarity relation (see the figure, panel **b**, in which the symbols are defined in equation (7) in the main text).

Interparticle interaction

In the dual-space method, one defines a bounding plane as $\{(x, y, z)|ax + by + cz = d\}$ for a convex polyhedron (see the figure, panel **c**). Mapping between a plane and a point in the dual space (the prime for variables in the image space) follows the relation[81,82]:

$$\mathbf{p} \Rightarrow \mathbf{p}' = \left(\frac{a}{d}, \frac{b}{d}, \frac{c}{d}\right), \mathbf{q}' \Rightarrow \mathbf{q} = \left(\frac{a'}{d'}, \frac{b'}{d'}, \frac{c'}{d'}\right)$$

One common optimization method (see the figure, panel **d**) is midway or potential optimization:

$$\text{minimize } S_1(\mathbf{x}) + S_2(\mathbf{x})$$
$$\text{subject to } S_1(\mathbf{x}) = S_2(\mathbf{x})$$

where $\mathbf{x}$ is the midway point and $S_1(\mathbf{x})$ and $S_2(\mathbf{x})$ are surface or potential functions of particles. Another widely used optimization method is common normal or support point optimization:

$$\text{minimize } |\mathbf{S}_2(-\mathbf{c}) - \mathbf{S}_1(\mathbf{c})|$$
$$\text{subject to } (\mathbf{S}_2(-\mathbf{c}) - \mathbf{S}_1(\mathbf{c})) \times \mathbf{c} = 0$$

in which $\mathbf{c}$ is the common normal and $\mathbf{S}_1(\mathbf{c})$ and $\mathbf{S}_2(\mathbf{c})$ are support functions of particles.

In the brute-force method, the interaction between each pair of primitives from two particles is traversed. The point-to-point traversal is a typical approach (see the figure, panel **e**). In addition, the node (point)-to-surface method is to query the penetration of a node from one particle into the other represented by a surface (see the figure, panel **f**). To facilitate the querying process, a level-set function or a general signed distance field (SDF) function is used to pre-cache the distance potential in a grid structure. See the figure, panel **g** for a level-set contour of a particle surface (the dot-dashed profile). An exemplified SDF of a particle represented by a mesh is shown (see the figure, panel **h**).

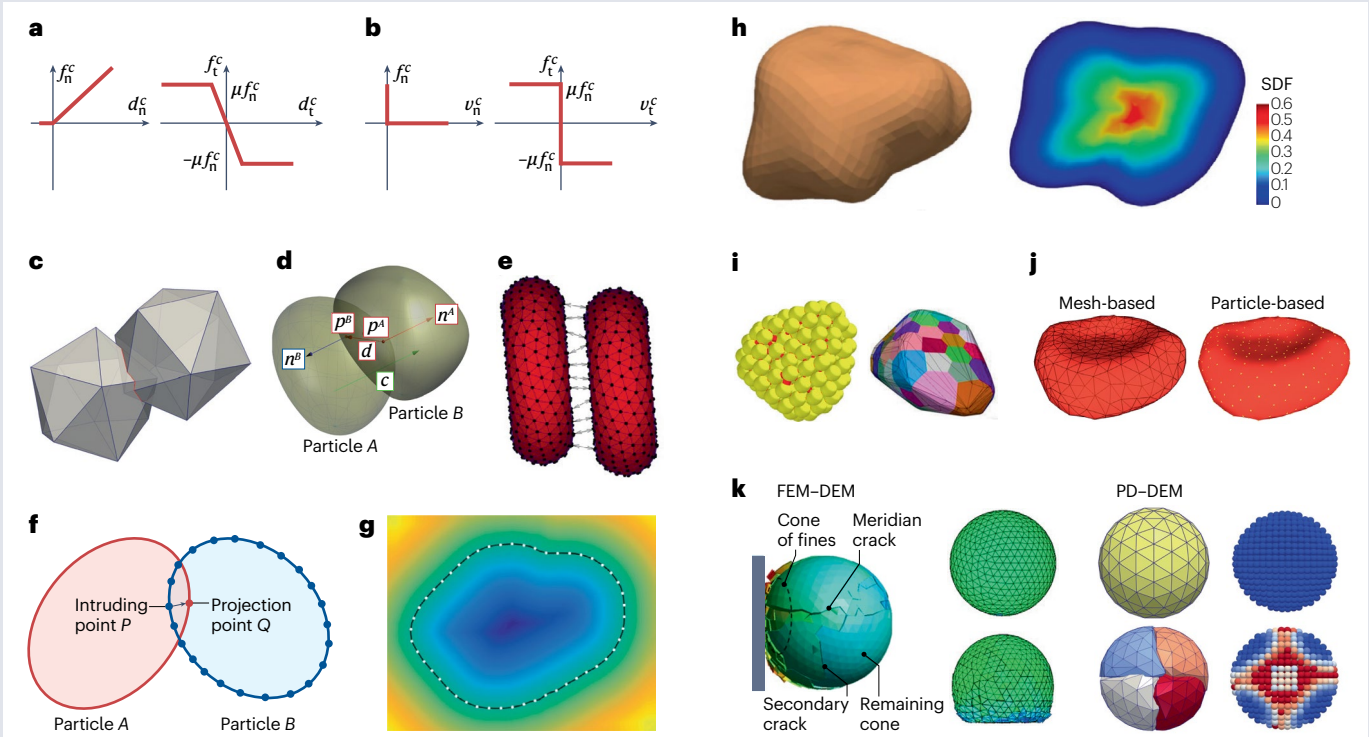

(continued from previous page)

Intraparticle interaction

In a discrete approach, particle shape is represented by using the primitive-clump scheme with primitives such as sphere and polyhedron. Intraparticle interaction between these primitives is modelled for particle deformation and crushing by the discrete element method (DEM) or molecular dynamics (see the figure, panel **i**).

In a continuum approach, particles are modelled as general continuum with intraparticle stress and strain governed by the linear momentum equation subject to boundary conditions, such as contact force or confinement. Either meshes or material points are used to discretize particle shape (see the figure, panel **j**), corresponding to the mesh-based methods such as finite element method (FEM) and the particle-based methods such as material point method, smoothed particle hydrodynamics and peridynamics (PD).

Intraparticle interaction with particle dynamics

Particle deformation or crushing path in an assembly can be tracked by either discrete methods (such as DEM) or continuum methods (such as material point method). Coupling continuum and discrete methods, such as in FEM–DEM and PD–DEM (see the figure, panel **k**), helps to leverage the advantages of both methods on the modelling of particle deformation or crushing.

Replacement model for particle crushing

In this model, the parent particle is replaced by an aggregation of small particles. The small particles can be generated empirically or with respect to a semiempirical population balance model. The 1D population balance model equation is given by

$$\frac{\mathrm{d}m_i}{\mathrm{d}t} = -K_i m_i + \sum_{j=1}^{i-1} b_{ij} K_j m_j = 0,\ i \in [1, N]$$

m_i is the particle mass fraction in size group of N groups, K_i is the breakage constant and b_{ij} is the breakage distribution parameter defining particle mass fraction formed in size group i from group j (ref. 112).

Part **c** adapted with permission from ref. 82, Springer. Part **d** adapted with permission from ref. 205, Elsevier. Part **e** adapted with permission from ref. 206, Elsevier. Part **f** adapted with permission from ref. 100, Springer. Part **g** adapted with permission from ref. 97, Elsevier. Part **h** adapted with permission from ref. 100, Springer. Part **i** adapted with permission from refs. 7,114, Elsevier. Part **k** adapted with permission from refs. 44,87, Elsevier.

drawback of the hierarchical grid is that it is problem-specific and requires a sophisticated data structure and is thus harder to implement than other methods. The overall performance of broad-phase detection algorithms can be improved by storing the neighbour list in cache and updating the potential neighbours of each particle[78,79].

Narrow-phase contact detection. Narrow-phase contact detection provides accurate resolution of interparticle contacts. There are general-purpose algorithms available for simple, spherical particles. However, there is no easy technique for accurate contact detection of particles with irregular or arbitrary convex or concave shapes, and relevant algorithms are often case-specific and problem-specific. Existing approaches can be classified into three categories: analytical, optimization-based and brute-force methods (Box 1).

The analytical method only works for simple primitives. For example, there is a closed-form analytical solution that can readily be coded for numerical simulations to calculate the minimum distance between two discs or two spheres. However, even slightly distorted shapes such as ellipsoids render such a solution unattainable. In the case of ellipsoids, the problem can be tackled in different ways[80]. Notably, the dual-space method is a promising method that has been successfully used in standard DEM[81,82] and offers a robust solution to the intersection between two convex polyhedra using dual spaces[83]. This method transforms the half-space planes of the contacting polyhedra into discrete points in the dual space and identifies the convex hull of those points as the intersection in real space. The intersection polyhedron facilitates determination of the contact volume to resolve the contact force in conjunction with the volumetric contact stiffness in standard DEM. The introduction of volumetric contact stiffness contributes further to numerical stability when developing an energy-conservative contact model[84]. Despite these good features, the dual-space method is computationally inefficient, especially for polyhedra with manyvertices.

The optimization-based method is applicable to any convex shape, from convex polyhedra to all convex shapes that are suitable for the analytical-surface scheme discussed earlier. Indeed, optimization-based methods are the contact resolution strategies for most convex particle shapes proposed in DEM today, including ellipsoids, superellipsoids[46,47], poly-superellipsoids[50], meta-balls[52] and convex Fourier-based shapes[85]. In standard DEM, the optimization problem is formulated to search a minimum distance between two particle surfaces, subject to constraints such as common normal direction. The problem is solved using suitable optimization algorithms such as the Nelder–Mead simplex algorithm, the Gilbert–Johnson–Keerthi (GJK) algorithm, Newton's method and the Levenberg–Marquardt algorithms. In some cases, the combined use of these optimization algorithms — such as a hybrid of Levenberg–Marquardt and GJK[50] — may help achieve better convergence. All the optimization algorithms mentioned earlier are equally applicable to CD and impulse-based DEM. Notably, GJK has been adopted widely in physics engines for computer graphics. Recently, physics engines such as PhysX[86] and Bullet[87] have become increasingly popular in scientific computation. For event-driven DEM or MD, it is non-trivial to predict the collision time for non-spherical moving particles[88]. The Donev–Torquato–Stillinger (DTS) algorithm[71] has been proposed to extend the Lubachevsky–Stillinger algorithm[89] to handle non-spherical particles with centrally symmetric convex shapes, such as ellipsoids and superballs[90]. With further simplification by assuming equal principal moment of inertia, the Donev–Torquato–Stillinger algorithm solves interparticle overlap potentials as an optimization problem.

The brute-force method is the most straightforward for resolving contacts between non-spherical particles modelled by clumped spheres in standard DEM or MD. It can also be used for shapes represented by the primitive-clumped scheme. This method determines possible contacts between each pair of primitives (for instance, spheres in the clumped spheres) of the two non-spherical particles to collect all

information for the contact. For the case of convex polyhedra, it is usual to adopt the common plane algorithm proposed by Cundall et al.[91], which has been extended by traversing a set of potential candidate common planes[92]. In addition, early studies of contact detection among polyhedra proposed approaches that traverse possible face–face, vertex–face and face–edge pairs[93]. However, such methods are not as computationally efficient as those based on optimization methods for convex shapes. For advanced shape-representation methods such as the mesh-based scheme and the analytical-surface scheme for arbitrary shapes, the primitives can be points (vertices), segments and triangles (or polygons). For example, if the vertex is used as primitive, it gives better performance than using a triangle as primitive[94] but may possibly cause some loss of accuracy for mesh-based shapes. The node-to-surface detection algorithm promises to address the issues in vertex–vertex or triangle–triangle contact detection and has been used for SH-based methods[57,95,96]. More recently, the level-set and signed-distance field (SDF) functions originally used in computer graphics are attracting increasing attention for application in advanced DEM to accelerate node-to-surface detection, such as level-set-based DEM[97–99] and SDF-based DEM[100–102].

Interparticle contact model. For smooth contact interactions, interparticle overlap is allowed, to compute contact forces. Penetration depth can be obtained during the narrow-phase contact detection and used as a weight or penalty for force calculations. However, contact models based on penetration depth may not be suitable for non-spherical particles as they can cause undesired behaviour for the system stiffness and damping when multiple contacts occur. As a result, contact models for general non-spherical particles are still being discussed. Energy-conserving contact models have been proposed to ensure numerical stability for non-spherical particles[103]. The volume-based contact model also falls into this category. Note that the volume-based contact model is commonly computationally expensive. Alternatively, for mesh-based shapes, the intersection line between two particles can be resolved instead of the overlap volume[84]. Moreover, both level-set and SDF functions can resemble a potential-based contact model[97,100]. For non-smooth contact interactions, although there are no stiffness-overlap relations directly to compute contact force, interparticle overlap is iteratively computed to ensure that particles are impenetrable according to a threshold value applied to overlap. Multiple contacts can also cause issues for non-spherical particles, resulting in excess complications for adjusting particle positions to maintain the complementarity condition. For clustered particles in which multiple contacts may occur, in addition to the induced excess friction and interlocking, multiple contacts need to be stored and the contact history has to be maintained at each contacting pair, which necessarily invokes higher memory and computational cost[39].

Crushable and deformable particles

Granular particles may deform negligibly or markedly when subjected to external loading and may also break slowly or suddenly under various conditions. Indeed, granular particle crushing is ubiquitous and is important in many industrial and natural processes, such as grain milling, chipping of pharmaceutical tablets, Li-ion particle crushing or asteroid collisions. Brittle particles may undergo sudden crushing at negligible deformation, whereas ductile or cohesive particles may show slower, smoother breakage processes. Both DNS and semi-empirical approaches have been developed to model the post-crushing child particles without tracking the entire crushing process. Meanwhile, in certain situations, granular particles may exhibit elastic and/or plastic deformations. Such deformations can be seen in red blood cells[104], artificial soft particles such as filled polymers in microgel particle suspensions[105] and flexible fibres in fluid[106], as well as powders, among other examples. Another example is the adaptation of the shape of granular hydrogels to adapt their mechanical properties for biomedical applications such as healing and cardiac repairs[107]. The following focuses mainly on DNS approaches to modelling crushable and deformable particles (Box 1).

Crushable particles

Semi-empirical approaches. Holistic treatments have been widely considered for modelling particle crushing, in view of the extreme complexity of grain crushing, which involves changes in both particle size and shape. A relatively intuitive method is the replacement approach, in which the original particle is replaced by a set of smaller particles (typically spheres) after crushing[108]. The crushing criterion is decided empirically from the overall contact force or other measures. However, such a simple replacement approach may lead to considerable loss of volume when spheres are used. Further refinements can be incorporated to consider cracks and other defects, such as the damage separation model[109] and the level-set splitting approach[98]. The fracture surfaces are generally simplified as planes according to the advanced overall breakage criterion such as the maximum principal stress, Tresca or von Mises criterion on the basis of the intraparticle static stress:

$$\sigma_{\mathrm{p}} = \frac{1}{V_{\mathrm{p}}} \sum_{c=1}^{N} \mathbf{l}^{c} \otimes \mathbf{f}^{c} \tag{8}$$

where V_{p} is the particle volume; $\mathbf{l}^{c}$ and $\mathbf{f}^{c}$ are branch vector and contact force at contact c, respectively. We do not refer to dynamic, energy breakage criteria here. Population balance modelling is a semi-empirical approach with simplified mechanical consideration of the particle crushing process used widely in chemistry and pharmaceutics[110,111]. Population balance modelling has recently been coupled with the replacement approach in DEM to better capture the mechanical process[112].

Discrete-based DNS. The clustered-sphere model is among the most straightforward discrete-based DNS methods. In it, a particle breaks along the interparticle contacts between the clustered spheres. Different variants of the clustered-sphere model have been developed by simply using other shapes, such as polyhedra, to replace spheres as the primitives, including the clustered-polyhedron model[113] and its extension based on Voronoi tessellation[114] (or bonded cell method[110] for both 2D[115] and 3D[116]). Such primitive-clustered approaches enable dynamic tracking of cracks but have the pitfall that the possible cracks can only pass through prescribed internal contacts between primitives. Increasing the resolution of primitives may help to mitigate this issue at the cost of computational efficiency. Frequently, these primitive-clustered approaches need to be coupled with general DEM to simulate particle crushing within a granular system. Alternative approaches exist, including the lattice element method, which is suitable for modelling crack propagation at quasi-static conditions for small displacement problems[117]. The lattice element method introduces bonds, such as springs or beams, to connect adjacent nodes at a regular or irregular lattice, allowing for the modelling of cracks by debonding adjacent nodes. It can be applied to modelling the failure of interparticle interfaces, such as those in cemented granular materials[118,119], and intraparticle failure such as wheat fragmentation[120].

Continuum-based DNS. Conventional finite element method (FEM) and advanced techniques such as extended FEM for solid cracking problems (such as phase-field-based FEM[121]) are equivalently applicable to modelling grain crushing. More recently, mesh-free methods such as peridynamics (PD), smoothed particle hydrodynamics (SPH) and material point method (MPM) (Table 1) have become popular for modelling particle crushing and can be combined with conventional approaches to modelling cracking, as is done in phase-field-based SPH[122], for example. Continuum methods have further been coupled with discrete modelling approaches to consider interparticle interactions, represented by prevailing coupling schemes such as FEM–DEM[44] or PD–DEM[87,123,124].

Deformable particles

Discrete-based DNS. To simulate deformable particles, special shape representations are required to characterize the shape changes. Deformable particles can be either shell-like or solid. For shell-like particles such as biomembranes and capsules, the primitive-clump scheme is predominantly used because of its flexibility. For example, it is possible to use spheres or point clouds to construct realistic complex shapes such as realistic biomembranes[125] and hinge-like nanostructures[126]. The interactions between the primitives are modelled using either discrete modelling approaches such as DEM and MD or specific models such as an energy-based deformable polygon model[127,128]. These approaches are equally applicable to solid particles but may be more computationally demanding in that case because of increasing numbers and complexity of primitives.

Continuum-based DNS. The deformation of individual particles can be solved by either mesh-based or mesh-free continuum-based approaches. The mesh-based approaches have a solid theoretical basis in continuum mechanics and represent particle shapes elegantly using various mesh-based discretization schemes, such as the thin-shell model for deformable capsules[129] based on FEM. However, mesh-based methods such as FEM may encounter the issue of mesh distortion when the particles experience excessively large relative deformation. Advanced techniques such as arbitrary Lagrangian–Eulerian (ALE) methods may help to mitigate the issue, but compromise computational efficiency and cause possible convergency issues. A single-element particle scheme[130] has been proposed to model flexible polyhedral particles on the basis of the virtual element method for better computational efficiency, but the scheme sacrifices accuracy. Emerging mesh-free approaches such as SPH and MPM are well suited to large-deformation problems (Table 1). Both SPH and MPM are particle-based methods. But unlike DEM, they solve continuum equations rather than the discrete particle motion. In these methods, deformable particles can be represented by point clouds. However, accurate representation necessarily requires substantial point clouds, causing great demand for computing resources and high computational cost. As such, continuum-based DNS approaches can at best be used for mesoscale modelling; they cannot replace discrete modelling approaches to atomic or microscale interactions, such as atomic interactions in the deformation of metal (nano) particles[131].

Interactions with deformable particles. Interparticle interactions for assemblies of deformable particle can be modelled using general discrete modelling approaches. Coupled schemes such as the coupling of FEM and DEM (FDEM or DEFEM)[132], CD–FEM[133] and CD–MPM[134,135] are popular examples. In addition to interparticle interaction, particles may be deformed by other forces such as fluid–particle interactions. Examples include red blood cells in vessels[104] and flexible fibres in fluid flows[106]. These latter interactions are detailed in the next section. Furthermore, the spontaneous deformation of artificial particles is an active topic of research, especially in the context of meta-materials, which goes beyond the scope of this Technical Review. One example is deformable nanoparticles with varying patterns of surface charge[136].

Particle–fluid interaction

Method overview

Computational fluid dynamics (CFD) is a prevailing method for direct numerical simulation (DNS) of fluid flow. Popular CFD methods are based on the finite volume method. The latest developments also see alternative CFD variants such as the lattice Boltzmann method (LBM) and SPH. Particle–fluid interactions have been treated as a fluid–solid coupling problem for which various emerging computational methods have been developed to treat specific problems involving non-spherical particles interacting with fluid[64].

Particles in fluid. Particle–fluid interactions can be modelled in either resolved or unresolved manners (Box 2). The resolved (or particle-resolved) approach solves the particle–fluid interaction at each discretized subsurface of a particle, whereas for the unresolved (or particle-unresolved) approach the particle–fluid interaction is solved approximately using empirical models. Whereas the former works with a resolution much smaller than the particle[137], the latter can be much faster owing to a much lower refinement[138]. Evidently, the resolved approach is directly applicable to non-spherical particles but inevitably incurs higher computational costs. The unresolved approach depends strongly on empirical fluid–particle interaction models such as drag force models, which are not readily available for non-spherical particles. For mesh-based fluid solvers, the finest Eulerian grid must be larger than the particles (for instance, at least three times larger than the particle) in the unresolved approach[139]. Particle–fluid interactions are then coupled with interparticle interactions solved using DEM[140,141] or other interparticle collision models[142] for particle-laden flows or sediment transport (refs. 64,139 provide more exhaustive reviews of these methods).

Microswimmers. Particle–fluid interactions may differ greatly when the scale is rather small, such as in Brownian motion[32]. Particles such as microplastics, colloidal particles, biocells and microorganisms are frequently referred to as microswimmers and comprise an active research topic for computational modelling[143]. Although microswimmers are commonly non-spherical, the primitive-clumped scheme in MD has proved to be effective and widely adopted, and the fluid is often modelled by a mesoscale method such LBM[144]. A point-friction coupling scheme[145] can be used to couple LBM with MD to model biological processes such as bacterial accumulation[146]. Moreover, DPD is also suitable for modelling microswimmers such as red blood cells moving in the blood flow[104].

Fluid in particles. For unsaturated granular materials, fluid (liquid) may be absorbed on the particle surface and form liquid layers or liquid bridges between particles, as in capillary condensation[147], for example. The aforementioned DNS approaches, whether resolved or unresolved, are inadequate for directly modelling fluid–particle interaction in such conditions[148]. The solution to this problem mandates further consideration of a multiphase fluid and its free surface, using a method

Box 2

Particle–fluid interaction for particles in fluid

Fluid dynamics

Fluid dynamics can be described by the incompressible Navier–Stokes equations:

$$\mathcal{N}(\mathbf{u}) = \rho(\partial_t + \mathbf{u}\cdot\nabla)\mathbf{u} + \nabla p - \mu\nabla^2\mathbf{u} = \mathbf{f}_d$$

$$\nabla\cdot\mathbf{u} = 0$$

in which ρ is the mass density, $\mathbf{u}$ is the velocity, p is the pressure, μ is the viscosity and $\mathbf{f}_d$ is the force density.

An alternative computational approach is to use the lattice Boltzmann equation:

$$f(\mathbf{x}+\mathbf{v}\Delta t|t+\Delta t) - f(\mathbf{x}|t) = -\frac{1}{\tau}(f(\mathbf{x}|t) - f^{eq}(\mathbf{x}|t))$$

in which $f(\mathbf{x}, t)$ is the particle distribution function at position $\mathbf{x}$ and time t, $f^{eq}(\mathbf{x}, t)$ is the equilibrium distribution function, $\mathbf{v}$ is the particle velocity and τ is a relaxation parameter.

Particle–fluid interaction

With respect to the interaction resolution, particle–fluid interaction can be particle-resolved or unresolved. Panel **a** (see the figure) refers to an unresolved case in which the fluid cell is typically several times bigger than the particle size and the particle–fluid interaction forces are holistically resolved and applied to the mass centre of each particle without considering their actual shape. Panel **b** (see the figure) refers to the resolved case in which the particle is typically bigger than the fluid cell. The particle surface is discretized to match the surrounding fluid mesh to resolve the interaction at each cell before summing them up to form the total interaction forces.

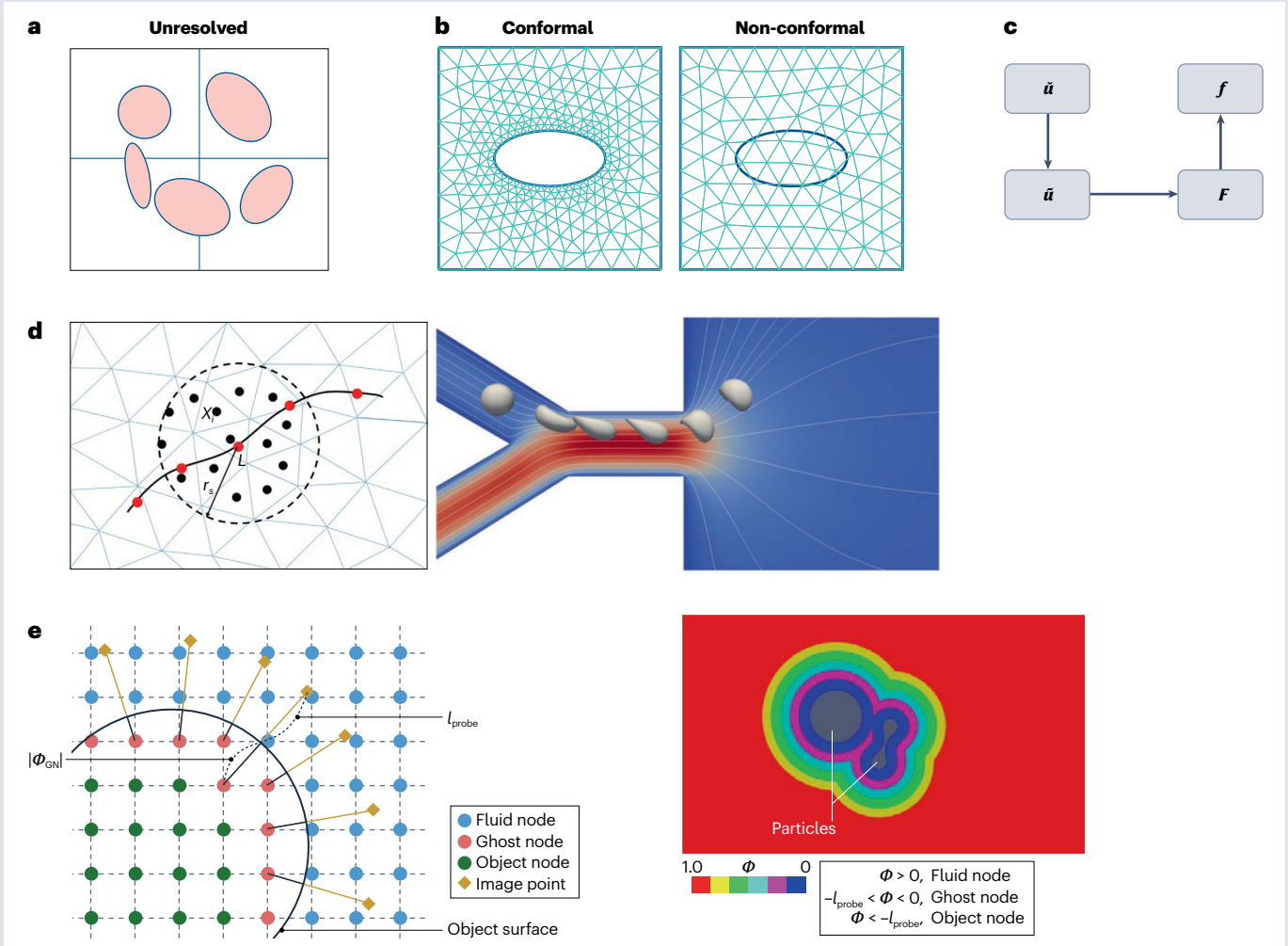

(continued from previous page)
For mesh-based solvers of fluids, the resolved approach can be boundary conformal or not (see the figure, panel **b**).

Variational formulations in distributed Lagrangian multiplier-based fictitious domain

These are given by

$$\int_{\Omega} \mathcal{N}(\mathbf{u}) \cdot \mathbf{v} \mathrm{d}\mathbf{x} + \sum_{i=0}^{n} \int_{P_i} \boldsymbol{\lambda} \cdot \mathbf{v} \mathrm{d}\mathbf{x} = 0,$$

$$\mathcal{L}_i - \sum_{c} \mathbf{f}^{c} \cdot (\mathbf{V}_i + \boldsymbol{\zeta}_i \times \mathbf{r}_i) - \int_{P_i} \lambda \cdot (\mathbf{V}_i + \boldsymbol{\zeta}_i \times \mathbf{r}) \mathrm{d}\mathbf{x} = 0,$$

$$\mathcal{L}_i = \left(1 - \frac{\rho_{\mathrm{f}}}{\rho_{\mathrm{s}}}\right)\left[m_i\left(\frac{\mathrm{d}\mathbf{U}_i}{\mathrm{d}t} - \boldsymbol{a}\right) \cdot \mathbf{V}_i + \frac{\mathrm{d}J_i\omega_i}{\mathrm{d}t} \cdot \boldsymbol{\zeta}_i\right],$$

$$\int_{P_i} \alpha \cdot (\mathbf{u} - (\mathbf{U}_i + \boldsymbol{\omega}_i \times \mathbf{r})) \mathrm{d}\mathbf{x} = 0,$$

where Ω is the entire domain; P_i is the domain of particle i; $\mathcal{N}(\mathbf{u})$ is the Navier–Stokes operator; $\boldsymbol{\lambda}$ is a Lagrangian multiplier vector; ρ_{f} and ρ_{s} are the densities of fluid and solid and $\mathbf{v}$, $\mathbf{V}$, $\boldsymbol{\zeta}$ and α are test functions for fluid velocity $\mathbf{u}$, particle velocity $\mathbf{U}$, particle angular velocity $\boldsymbol{\omega}$ and λ.

Discrete forcing immersed boundary method

In discrete direct forcing, spatial discretization is not modified near the immersed boundary. The forcing is directly calculated from the discrete form of Navier–Stokes equation:

$$\mathbf{f} = \rho\frac{\mathbf{V}_{\mathrm{ib}} - \mathbf{u}}{\Delta t} + \rho(\mathbf{u} \cdot \nabla)\mathbf{u} + \nabla p - \mu\nabla^2\mathbf{u},$$

where $\mathbf{V}_{\mathrm{ib}}$ is the velocity of the immersed boundary (Lagrangian points). For arbitrarily moving particles, a direct application of the aforementioned equation may potentially cause strong oscillation in hydrodynamic forces. To mitigate this issue, the two-step forcing by Uhlmann[157] (see the figure, panel **c**) is widely used:

$$\mathbf{F} = \rho\frac{\mathbf{V}_{\mathrm{ib}} - \tilde{\mathbf{u}}}{\Delta t}$$

$$\mathbf{f}(\mathbf{x}) = \sum_{\mathbf{X} \in U} \mathbf{F}(\mathbf{X})\delta_h(\mathbf{x} - \mathbf{X})\Delta U$$

$$\tilde{\boldsymbol{u}}(\mathbf{X}) = \sum_{\mathbf{x} \in U} \check{\boldsymbol{u}}(\mathbf{x})\delta_h(\mathbf{x} - \mathbf{X})\Delta U$$

in which $\mathbf{F}$ and $\tilde{\mathbf{u}}$ are force and fluid velocity at Lagrangian points, respectively; $\check{\mathbf{u}}$ is the provisional fluid velocity without forcing and δ_h is the regularized delta function (in which the subscript h is affixed to distinguish it from the standard delta function δ). The usage of δ_h causes smooth velocity gradient near the boundary. See the figure, panel **d** for an example.

Alternatively, one can impose boundary conditions on ghost cells that are inside the solid domain with neighbours in the fluid domain; the ghost cells can be flagged by techniques such as level-set methods[207] (see the figure, panel **e**). This approach can capture gradient discontinuity but does not satisfy local mass conservation or even momentum conservation.

In a cut cell approach, boundary cells are cut to satisfy the conservation laws, but doing so is challenging and computationally expensive for 3D and moving particles. GN, ghost node.

Part **d** adapted with permission from ref. 129, AIP. Part **e** adapted with permission from ref. 207, Wiley.

such as multicomponent LBM[149]. Accurate simulation of fluid–particle interaction in these conditions requires more advanced and complex approaches that consider the complexities of multiphase fluids in the presence of non-spherical particles. Mesoscale approaches such as mDPM use fluid parcels much larger than atoms as a compromise between accuracy and performance[33]. When the fluid–particle interaction is dominated by the capillary force, it can be solved using the Young–Laplace equation instead of DNS. For non-spherical particles, the local curvature at the contact point can be used as an approximation to solve the liquid bridge force. The liquid transfer between particles can be estimated using analytical models at low computational cost[150].

Mesh-based resolved approach

Boundary-conformal and boundary-non-conformal approaches. To resolve particle–fluid interactions properly, it is essential that a resolved approach tracks the particle–fluid interface or boundary. Mesh-based CFD commonly adopts boundary-conformal (or body-fitted) methods to handle the particle–fluid interface accurately. A representative method is the ALE method, in which the fluid Euler grid conforms with the particle surface to handle the particle–fluid interface accurately with no-slip boundary conditions readily imposed directly. However, when applied to moving particles, such methods may suffer from frequent grid regeneration or re-meshing. By contrast, non-boundary-conformal methods keep a fixed fluid grid (Eulerian mesh) with movable and/or deformable particles (Lagrangian or material points) superimposed. A typical direct approach is to use overlapping grids with the ALE formulation, such as in the moving non-conforming Schwarz-spectral element method[151].

Fictitious domain method. The fictitious domain (FD) method is another prevailing boundary-non-conformal approach. It refers to a class of techniques to find the solution of partial differential equations with complex geometries embedded in a larger domain. For the specific case of particle–fluid interaction, the fluid domain occupied by solid particles is taken as the FD. A typical FD method is the distributed Lagrangian multiplier (DLM) method that incorporates the no-slip condition into the variational formulation of the conservation equations using Lagrangian multipliers (Box 2). In DLM-based FD, the hydrodynamic forces acting on particles are not solved directly; as a result, DLM-based FD is also known as the implicit fictitious boundary method (FBM). DLM-based FD has also been coupled with phase-field methods to consider a two-phase fluid[152]. The explicit FBM[153] uses a multigrid finite element method with hydrodynamic forces obtained directly by volume integration. Both DLM-based

FD and FBM are limited to 2D simulations because of their excessive computational cost.

Immersed boundary method. The immersed boundary method (IBM)[154] belongs to another category of FD approaches. It only considers the particle surface domain and is more computationally efficient. Note that researchers may distinguish IBM from FD in the literature[155,156]. IBM came first and as originally proposed with a regularized Dirac delta function to exchange velocity and force between the Lagrangian markers of a particle and the Eulerian nodes of a fluid grid. With advanced variants such as the direct forcing approach[157], IBM has become a canonical technique to tackle resolved particle–fluid interactions for moving arbitrarily shaped particles including thin membranes[158]. There are two categories of IBM, different in how they implement the forcing term ($\mathbf{f}_d$ and $\mathcal{N}(\mathbf{u})$ in Box 2) for an immersed body. One is continuous forcing, in which $\mathbf{f}_d$ is directly introduced in the governing equations (that is, $\mathcal{N}(\mathbf{u}) = \mathbf{f}_d$), which are then discretized over the whole domain. The other is discrete forcing that introduces the forcing term in the vicinity of the immersed body after discretizing the governing equations (that is, $\mathcal{N}(\mathbf{u}) = 0$). Continuous forcing has formulations independent of spatial discretization, and the velocity gradient is smoothed by a finite-width regularized delta function. Discrete forcing is generally more flexible and accurate with specific techniques including the direct forcing method, ghost cell method and cut cell method (Box 2). Similar to the direct forcing IBM, there is another simple and efficient approach called the smoothed profile method that[159] uses smoothed profiles to replace particle–fluid interfaces of shapes, which is suitable for sphere-clumped particles.

Particle-based resolved approach

As summarized in Table 1, particle-based approaches such as LBM, SPH, MPM and DPD can be used to solve fluid dynamics.

LBM. LBM models fluid dynamics by solving the lattice Boltzmann equation at the mesoscale rather than directly tackling the Navier–Stokes equations; in conventional CFD, it uses methods such as the finite volume method[160]. Coupling LBM with IBM to solve complex fluid–particle interaction problems is considered promising and has been applied to simulate particle flow in areas such as microfluidics[161]. Coupling challenges such as small amplitude perturbations during wave propagation in saturated granular media have also recently been tackled by LBM[162].

SPH and MPM. SPH is a Lagrangian-based approach solving the Navier–Stokes equation for fluid flow[163]. Particles are represented as a collection of SPH particles in a similar manner as the primitive-clump scheme, thereby avoiding the need for ad hoc boundary treatment for particle–fluid interaction. Nevertheless, the density jump at the particle–fluid interface may cause a substantial gap between fluid and solid particles that needs further corrections[164]. SPH also works for solid or soil mechanics and is well suited to simulating deformable particles. Instead of discretizing the whole particle, multilayer ghost–fluid particles can be attached to the solid particle[165]. Moreover, a penalty-based contact scheme analogous to DEM is applicable to the interaction between SPH particles and solid particles[166,167]. Nevertheless, the spring–damper parameters introduced in the method remain somewhat artificial.

MPM became fashionable a little later than SPH and avoids several of its problems, allowing for a much more rigorous solid-mechanics treatment of the particles. Theoretically, the same fluid–particle interaction strategy in SPH can also be applied to MPM, via the penalty-based scheme[168], for example. However, moderate differences may be observed in their implementation. For example, the interface boundary condition in MPM can also be applied on the background grid in addition to material points.

DPD. Unlike SPH and MPM, DPD can be considered as a coarse-grained MD method, which models fluid flows at the mesoscale[169] that involves temperature and Brownian motion. It has been widely adopted to simulate biomembranes and suspensions, such as red blood cells[104], in which both the fluid and cells are modelled by DPD particles without requiring ad hoc treatment of fluid–particle (cell) interactions.

Unresolved approach

The unresolved approach simplifies the particle–fluid interaction to a body force that can readily be incorporated into Newton's equation for particle motion and the Navier–Stokes equation for fluid flow. This approach works well for spherical particles, but it remains challenging for non-spherical particles because of a lack of robust and flexible empirical models to describe the interaction body forces accurately, especially the drag force. Efforts have been devoted to establishing either a specific model for a particular particle shape (such as microplastic fibres[170]) or a unified model for arbitrary shapes[171]. However, it is non-trivial to establish a unified model that must quantify particle shape using simplified descriptors such as sphericity[172] and aspect ratio[173]. Direct numerical simulations[173–175] have also been adopted to investigate the effect of particle shape on the drag and lift coefficients on the basis of resolved approaches. Further consideration of turbulent wakes by delayed-detached eddy simulation models[176] may help to establish more sophisticated empirical models for the unresolved approach. However, many studies involve single or several particles with oversimplified surrounding fluid conditions for calibration purpose only[177], a scenario that is beyond the scope of this Technical Review.

Large-scale and multiscale modelling

Direct numerical simulation

Table 2 summarizes the representative computational approaches for granular matter with non-spherical particles. The realistic simulation of particle shape necessarily results in a high demand for computing resources, especially for large-scale simulations. Indeed, large-scale simulations of spherical granular matter are already commonplace for industrial processes and engineering practices. The various techniques of DNS described earlier may not be directly applicable to large-scale simulations involving many particles with complicated shapes. Various techniques have been developed to tackle the challenge, including coarse-grained modelling and continuum–discrete modelling approaches (Fig. 3). The continuum–discrete coupling approach has become popular for multiscale modelling. Specifically, continuum-based methods such as FEM, SPH and MPM are coupled with discrete-based methods such as DEM and MD in a hierarchical or concurrent manner, leveraging the advantages of both methods to solve different engineering problems by running full resolution only where necessary (in space or time).

Coarse-grained modelling. Coarse-grained modelling uses larger particles to replace particle groups or clustered particles, while retaining equivalent collective (bulk) responses. It is effective for

Table 2 | Representative computational approaches for granular matter with non-spherical particles

Problem	Method	Description
Shape representation: modelling particle shapes with varying resolution	Primitive-clumped scheme	Primitives can be points, discs, spheres, cylinders and so on. Many primitives are required to approximate a realistic complex shape with high resolution. Suitable for solving intraparticle interactions
	Mesh-based scheme	Triangular mesh or its Minkowski sum with a sphere. The most flexible approach for representing a realistic complex shape. Can be more efficient than the primitive-clumped scheme
	Analytical-surface scheme	Ellipsoids, poly-ellipsoids, superellipsoids, poly-superellipsoids, NURBS, spherical harmonics and so on. Can be the most efficient when using optimization algorithms with frame cohesion in simulations
Interparticle contact interactions, which depend on particle shapes	Analytical method	Limited application for non-spherical shapes. The dual-space method works only for convex polyhedral, but it is considerably inefficient with increasing vertex number
	Optimization-based method	Suitable for convex shapes with optimization algorithms such as Nelder–Mead simplex, GJK and LM algorithms. Convex polyhedral and analytical-surface particles are preferable. Can be the most efficient with frame cohesion
	Brute-force method	General for arbitrarily shaped particles. Suitable for the primitive-clumped and mesh-based shapes. Less efficient than the optimization-based method. Neighbour-list algorithms can be applied to primitives for better performance
Intraparticle interaction: interaction within a particle that can deform and/or crush under external loading at the surface	Semi-empirical approach	Replacement approach, damage separation model, level-set splitting approach, PBM and so on. Most efficient but in sacrifice of accuracy
	Discrete-based DNS	Clustered-sphere, clustered-polyhedron, bonded cell approaches based on DEM. LEM is also applicable but suitable for quasi-static conditions with small displacement problems
	Continuum-based DNS	Mesh-free methods such as SPH, MPM and PD are superior to mesh-based ones. Can handle interparticle contacts with proper contact implementation or coupling with DEM such as CD–MPM and PD–DEM
Particle–fluid interactions	Mesh-based resolved approach	Boundary-conformal methods such as ALE are computationally intensive; boundary-non-conformal methods such as FD are more flexible and efficient. The discrete forcing variant of IBM is widely used
	Particle-based resolved approach	LBM, SPH, MPM and DPD as particle-based fluid solvers are popularly adopted, in which DPD is specifically suitable for microfluid flow. LBM is the most efficient for parallel computing owing to its lattice structure
	Unresolved approach	Particle–fluid interaction is captured by a holistic model. Far more efficient than the resolved approach but in sacrifice of accuracy. No elegant model for general arbitrarily shaped particles yet

ALE, arbitrary Lagrangian–Eulerian; CD, contact dynamics; DEM, discrete element method; DNS, direct numerical simulation; DPD, dissipative particle dynamics; FD, fictitious domain; GJK, Gilbert–Johnson–Keerthi; IBM, immersed boundary method; LBM, lattice Boltzmann method; LEM, lattice element method; LM, Levenberg–Marquardt; MPM, material point method; NURBS, non-uniform rational B-splines; PBM, population balance model; PD, peridynamics; SPH, smoothed particle hydrodynamics.

modelling macromolecules in MD and can readily be coupled with mesoscopic models to simulate large-scale systems, such as realistic biomembranes[125,178]. The idea of coarse graining has been extended to direct mesoscopic modelling, such as modelling red blood cells in DPD[104]. Coarse-grained modelling has more recently become popular to simulate the mechanical responses of granular materials by DEM[179] and modelling the multiphysics processes involving CFD[180].

A major issue with this method is the determination of upscaling laws and the inevitable system errors it introduces because of scale effects. Notably, the interaction between coarse-grained particles is simply an approximation of that between two groups of real particles. Moreover, the coarse-grained interactions may not capture the energy dissipation that occurs at interparticle contacts within a group. This limitation highlights the need for careful consideration when using coarse-grained modelling, as the accuracy of the model may be compromised by the assumptions made during the process of simplifying the system. It may become even more complicated when arbitrarily shaped particles with multiple contacts are modelled. Indeed, it remains an open question how much detail in particle shape, if any, is needed for a coarse-grained approach. Because the coarse grains model groups of particles, the shape detail of the primary objects may be smeared out in the coarse graining and become less important when it is projected into the much larger-scale interaction rules between the coarse particles. Meanwhile, it remains challenging for coarse-grained modelling to choose appropriate resolved or unresolved approaches to simulate particle–fluid interactions.

Continuum–discrete modelling. The continuum–discrete coupling approach has two representative variants: concurrent coupling and hierarchical coupling. For the concurrent approach, the simulation domain of interest is modelled by using discrete modelling approaches, whereas the remainder is simulated by continuum-based methods using conventional phenomenological material models. One critical challenge is to exchange physical properties and mechanical responses at the interface between the two subdomains, in which buffer zones are commonly considered. Great effort has been applied to this topic[179,181]. In the hierarchical coupling approach, no concurrent subdomains are considered. The entire domain is discretized by a continuum-based approach for which the required material responses are modelled and fed by high-resolution discrete-based methods, typically at each material point. This approach has been used successfully for the hierarchical multiscale modelling of granular materials, in terms of various coupling formulations such as FEM–DEM coupling[182,183] and MPM–DEM coupling[184,185], in which the DEM-simulated responses

provide a constitutive relation for FEM or MPM, thereby bypassing the necessity for the phenomenological constitutive models required in conventional continuum modelling. Moreover, it is possible to adopt hybrid coupling of both concurrent and hierarchical approaches for a boundary value problem or other variations thereof.

Machine learning

It is possible to leverage the advantage of ML in modelling granular matter. At the particulate scale, the direct use of ML techniques ranges from shape recognition, characterization[186,187] and contact resolution[188,189], to multiphysics fields such as particle–fluid interaction[190,191]. Particle

Fig. 3 | Computational approaches for large-scale and multiscale modelling. **a**,**b**, Coarse-grained modelling. **a**, Star polymer molecules are coarse-grained by simple spheres. **b**, Proteins on a bio-membrane are coarse-grained by arc-shaped particles. **c**, Hierarchical modelling across nanoscale and mesoscale. The figure shows exemplified hierarchical modelling of bio-membranes, where all-atom MD (aaMD), coarse-grained MD (cgMD) and mesoscale methods such as DPD can be bottom-to-up coupled. **d**, Continuum–discrete hierarchical modelling. The figure shows an exemplified coupling of material point method (MPM) and discrete element method (DEM), in which each material point of MPM corresponds to a DEM RVE, bypassing the conventional constitutive model in MPM. **e**,**f**, Continuum–discrete concurrent modelling. **e**, A reconciliation zone is required to exchange the response between the continuum and discrete regions or domains. The discrete modelling approaches such as DEM and MD are used for the particle region (discrete domain), whereas the continuum domain can be modelled by either mesh-based methods such as FEM or particle-based methods such as MPM (the left and right panels in part **f**). **g**,**h**, Machine learning (ML). **g**, An implicit mapping between experimental data and their characteristics. The figure shows an example of extracting characteristics of particle morphology by ML. **h**, Training advanced ML models for complex problems such as fluid flows within porous media as exemplified here requires a large set of data including DNS data. CFD, computational fluid dynamics; DE, discrete element; DNS, direct numerical simulation; FE, finite element; LBM, lattice Boltzmann method; MD, molecular dynamics; RVE, representative volume element; CNN, convolutional neural network. Part **a** adapted with permission from ref. 169, AIP. Part **b** adapted with permission from ref. 178, RSC. Part **c** adapted with permission from ref. 125, Elsevier. Part **d** adapted with permission from ref. 204, Springer. Part **e** adapted with permission from ref. 181, ACM. Part **f** adapted with permission from ref. 179, Elsevier, and ref. 181, ACM. Part **g** adapted with permission from ref. 187, Elsevier. Part **h** adapted with permission from ref. 194, Elsevier.

interaction models can be readily calibrated (see ref. 192 and references therein), in which not only additional information such as correlations between the microparameters but also micro–macro correlations are provided. Nevertheless, it remains an open issue whether considerable improvements in computational efficiency can be achieved, especially for contact resolution. At the mesoscopic scale, the physical and mechanical properties of an assembly can be trained into prediction models, for instance, by training constitutive response as a surrogate model to replace conventional constitutive models in continuum-based numerical methods[193]. Although there has been recent progress in applying data-driven[194] and physics-informed[195] techniques to obtain improved learning performance, ML approaches still need ground-truth data that are most often synthesized by DNS. A more promising direction for ML is to solve partial differential equations directly for large-scale simulations without having to use DNS.

Parallel computing

Particle-based numerical methods, including both discrete-based (such as DEM and MD) and continuum-based (such as SPH and MPM) methods, are well suited for parallel computing. Conventional CPU computing with shared memory and message passing interface parallelization has been successfully applied, for example, in modelling polyhedral particles[196] in DEM and coupled CFD–DEM[197]. Graphics processing unit (GPU) computing has attracted major attention across many disciplines owing to the tremendous increase in computing efficiency in the past decade. The resolution of interparticle interactions is the most computationally demanding part of these particle-based methods, especially for non-spherical particles and *N*-body problems[76]. In the case of the primitive-clumped and mesh-based shapes, primitive pairs can be resolved in parallel, rendering the simulation more efficient. In addition to the general GPU computing shaders, the emerging ray-tracing cores have also been used to accelerate interparticle collision detection[77]. Nevertheless, the performance of GPU computing suffers from communication bottlenecks and high energy consumption. Other energy-efficient hardware such as field-programmable gate array (FPGA)[198] may become an alternative in the future.

Outlook

Computational modelling approaches, purely particle or discrete-based, continuum-based or coupled methods, are a fast-growing body of research and allow tackling emerging challenges for granular matter in both engineering and science. Core to these approaches are the underpinning roles played by accurate characterization, representation and implementation of realistic particle shape. Such models offer versatile, robust means for high-fidelity and high-resolution simulation of granular matter. However, challenges remain for future realistic particle modelling.

The shape of granular particles is multiscale in nature and relevant in almost all industrial or natural granular systems. Particle shape modelling is problem-dependent and application-dependent and is usually limited by factors such as available information and affordable computing resources. Although some issues can be overcome by effective contact algorithms suitable for non-spherical objects, other physical properties of granular materials, including friction, cohesion, adhesion, dissipation and conformation, may require more accurate considerations of particle surface roughness or even finer scales. The straightforward primitive, analytical or mesh-based shape representations all need to be extended substantially to incorporate important information about the finer scales to render the bulk (multiparticle) simulations physically reasonable and more reliable. In addition to purely geometric descriptions, shape modelling for many granular systems may have to be extended by statistical physics or reduced-order modelling approaches to obtain reliable predictions in an efficient way.

There is a class of granular matter problems in which the particles may undergo transitions between hard and soft (deformable) states when the environment changes (such as changes in pressure or temperature[199]). Many numerical models have been developed for either hard or deformable particles, exclusively, without being able to account for possible transition processes and a hard–soft mix[200]. It is desirable to develop unified computational models that can consider the possible two-way transitions flexibly and handle the mixing of hard and soft particles robustly following effective contact detection. Further complications may arise if such transitions manifest as phase transformations (ordering, segregation or melting from solid to liquid, for example) or are coupled with further multiphysics fields.

Indeed, granular matter is a highly interdisciplinary research area pertaining to practical applications in which granular particles are subject to more diverse fields than ever, including thermal, hydraulic, mechanical, chemical, electromagnetic, photonic, active bio-matter fields and even architecture[21]. Accurately modelling the complex coupling between shape changes of particles and phase transformations and these environmental multiphysics fields is important for many scientific and industrial processes but is challenging to tackle. In fields such as civil engineering, it is critical to accurately model and

evaluate the shape effects in soil and rock mechanics, to better understanding the behaviour of natural hazards such as avalanches, debris flows, flooding, sediment transport and dust storm movements. These phenomena remain to be fully explored.

Meanwhile, it is worth noting that large-scale simulations of granular matter typically require considerable computing resources and computational time. The pertaining electricity consumption should never be underestimated and need to be fully considered in the development of various computational models mentioned earlier. Indeed, it has become an emerging scientific area to develop forward-looking interfaces between scientific computing and environmental sustainability. Energy-efficient computing systems, such as the FPGA machines, are increasingly used in scientific computing. Their widespread adoption remains limited by the computational efficiency they presently offer. The challenge can only be effectively addressed by developing numerical tools and software that can fully leverage the architecture of these advanced energy-efficient computing systems, to offer integrated solutions to energy-efficient computing also for granular matter. High-fidelity, high-efficiency computational modelling of granular materials integrated with environmental awareness design is a bright future prospect.

Finally, there are some fundamental questions to be answered regarding non-spherical particles. It is evident that methods and tools are available for fine-detail experimental observations and numerical modelling of non-spherical particles. How much detail is needed to solve a specific problem? Or to what extent will simplified shapes such as sphere suffice to provide satisfactory solutions? There are no uniform answers for these questions, and the criteria can be problem-specific and situation-specific. Future effort on granular matter modelling should also be devoted to comparison and understanding of simplified and detailed particle models to guide users on better model selection.

Published online: 10 August 2023

References

1. Marzinek, J. K., Huber, R. G. & Bond, P. J. Multiscale modelling and simulation of viruses. *Curr. Opin. Struct. Biol.* **61**, 146–152 (2020).
2. Zong, Y. & Zhao, K. Manipulation of self-assembled structures by shape-designed polygonal colloids in 2D. *Curr. Opin. Solid State Mater. Sci.* **26**, 101022 (2022).
3. Voss, J. & Wittkowski, R. On the shape-dependent propulsion of nano- and microparticles by traveling ultrasound waves. *Nanoscale Adv.* **2**, 3890–3899 (2020).
4. Wang, J. et al. Shape matters: morphologically biomimetic particles for improved drug delivery. *Chem. Eng. J.* **410**, 127849 (2021).
5. Luo, X., Wang, Z., Yang, L., Gao, T. & Zhang, Y. A review of analytical methods and models used in atmospheric microplastic research. *Sci. Total Environ.* **828**, 154487 (2022).
6. Mollon, G. & Zhao, J. Generating realistic 3D sand particles using Fourier descriptors. *Granul. Matter* **15**, 95–108 (2013).
7. Su, Y. et al. Determination and interpretation of bonded-particle model parameters for simulation of maize kernels. *Biosyst. Eng.* **210**, 193–205 (2021).
8. Ghadiri, M. et al. Cohesive powder flow: trends and challenges in characterisation and analysis. *KONA Powder Part. J.* https://doi.org/10.14356/kona.2020018 (2020).
9. Piton, G., Goodwin, S. R., Mark, E. & Strouth, A. Debris flows, boulders and constrictions: a simple framework for modeling jamming, and its consequences on outflow. *J. Geophys. Res. Earth Surf.* **127**, e2021JF006447 (2022).
10. Rackow, T. et al. A simulation of small to giant Antarctic iceberg evolution: differential impact on climatology estimates. *J. Geophys. Res. Ocean* **122**, 3170–3190 (2017).
11. Ferrari, F. & Tanga, P. The role of fragment shapes in the simulations of asteroids as gravitational aggregates. *Icarus* **350**, 113871 (2020).
12. Shi, L., Zhao, W., Sun, B. & Sun, W. Determination of the coefficient of rolling friction of irregularly shaped maize particles by using discrete element method. *Int. J. Agric. Biol. Eng.* **13**, 15–25 (2020).
13. Cui, X., Gui, N., Yang, X., Tu, J. & Jiang, S. Analysis of particle shape effect on the discharging of non-spherical particles in HTR-10 reactor core. *Nucl. Eng. Des.* **371**, 110934 (2021).
14. Tang, X. & Yang, J. Wave propagation in granular material: what is the role of particle shape? *J. Mech. Phys. Solids* **157**, 104605 (2021).
15. Jones, R. P., Ottino, J. M., Umbanhowar, P. B. & Lueptow, R. M. Predicting segregation of nonspherical particles. *Phys. Rev. Fluids* **6**, 054301 (2021).
16. Xia, Y. et al. Assessment of a tomography-informed polyhedral discrete element modelling approach for complex-shaped granular woody biomass in stress consolidation. *Biosyst. Eng.* **205**, 187–211 (2021).
17. Zhang, R., Ku, X., Yang, S., Wang, J. & Fan, L. Modeling and simulation of the motion and gasification behaviors of superellipsoidal biomass particles in an entrained-flow reactor. *Energy Fuels* **35**, 1488–1502 (2021).
18. Leisner, A. M., Richardson, D. C., Statler, T. S., Nichols, W. & Zhang, Y. An extended parameter space study of the effect of cohesion in gravitational aggregates through spin-up simulations. *Planet. Space Sci.* **182**, 104845 (2020).
19. Wang, F., Liu, J. & Zeng, H. Interactions of particulate matter and pulmonary surfactant: implications for human health. *Adv. Colloid Interface Sci.* **284**, 102244 (2020).
20. Wang, Y., Li, L., Hofmann, D., Andrade, J. E. & Daraio, C. Structured fabrics with tunable mechanical properties. *Nature* **596**, 238 (2021).
21. Keller, S. & Jaeger, H. M. Aleatory architectures. *Granul. Matter* **18**, 29 (2016).
22. Dierichs, K. & Menges, A. Designing architectural materials: from granular form to functional granular material. *Bioinspir. Biomim.* **16**, 065010 (2021).
23. Nunzi, F. & Angelis, F. D. Modeling titanium dioxide nanostructures for photocatalysis and photovoltaics. *Chem. Sci.* **13**, 9485–9497 (2022).
24. Ostanin, I., Ballarini, R., Potyondy, D. & Dumitrică, T. A distinct element method for large scale simulations of carbon nanotube assemblies. *J. Mech. Phys. Solids* **61**, 762–782 (2013).
25. Gentili, D. & Ori, G. Reversible assembly of nanoparticles: theory, strategies and computational simulations. *Nanoscale* **14**, 14385–14432 (2022).
26. Li, Z., Yang, F. & Yin, Y. Smart materials by nanoscale magnetic assembly. *Adv. Funct. Mater.* **30**, 1903467 (2020).
27. Sveinsson, H. A. et al. Direct atomic simulations of facet formation and equilibrium shapes of SiC nanoparticles. *Cryst. Growth Des.* **20**, 2147–2152 (2020).
28. Espinosa, I. M. P., Jacobs, T. D. B. & Martini, A. Atomistic simulations of the elastic compression of platinum nanoparticles. *Nanoscale Res. Lett.* **17**, 96 (2022).
29. Voss, J. & Wittkowski, R. Propulsion of bullet- and cup-shaped nano- and microparticles by traveling ultrasound waves. *Phys. Fluids* **34**, 052007 (2022).
30. Wang, C. & Jiang, H. Different-shaped micro-objects driven by active particle aggregations. *Soft Matter* **16**, 4422–4430 (2020).
31. Chen, G. et al. Liquid-crystalline behavior on dumbbell-shaped colloids and the observation of chiral blue phases. *Nat. Commun.* **13**, 5549 (2022).
32. Palanisamy, D. & den Otter, W. K. Intrinsic viscosities of non-spherical colloids by Brownian dynamics simulations. *J. Chem. Phys.* **151**, 184902 (2019).
33. Chakrapani, T. H., Bazyar, H., Lammertink, R. G. H., Luding, S. & Otter, W. Kden The permeability of pillar arrays in microfluidic devices: an application of Brinkman's theory towards wall friction. *Soft Matter* **19**, 436–450 (2023).
34. Schoenhoefer, P. W. A., Marechal, M., Cleaver, D. J. & Schroeder-Turk, G. E. Self-assembly and entropic effects in pear-shaped colloid systems. II. Depletion attraction of pear-shaped particles in a hard-sphere solvent. *J. Chem. Phys.* **153**, 034904 (2020).
35. Rosenberg, M., Dekker, F., Donaldson, J. G., Philipse, A. P. & Kantorovich, S. S. Self-assembly of charged colloidal cubes. *Soft Matter* **16**, 4451–4461 (2020).
36. Mistry, A., Heenan, T., Smith, K., Shearing, P. & Mukherjee, P. P. Asphericity can cause nonuniform lithium intercalation in battery active particles. *ACS Energy Lett.* **7**, 1871–1879 (2022).
37. Li, L., Wang, J., Yang, S. & Klein, B. A voxel-based clump generation method used for DEM simulations. *Granul. Matter* **24**, 89 (2022).
38. Huet, D. P., Jalaal, M., van Beek, R., van der Meer, D. & Wachs, A. Granular avalanches of entangled rigid particles. *Phys. Rev. Fluids* **6**, 104304 (2021).
39. Feng, Y. T. Thirty years of developments in contact modelling of non-spherical particles in DEM: a selective review. *Acta Mech. Sin.* **39**, 722343 (2023).
40. Neto, A. G. & Wriggers, P. Discrete element model for general polyhedra. *Comput. Part. Mech.* **9**, 353–380 (2022).
41. Zhang, R., Ku, X. & Lin, J. Fluidization of the spherocylindrical particles: comparison of multi-sphere and bond-sphere models. *Chem. Eng. Sci.* **253**, 117540 (2022).
42. Alonso-Marroqun, F. Spheropolygons: a new method to simulate conservative and dissipative interactions between 2D complex-shaped rigid bodies. *Europhys. Lett.* **83**, 14001 (2008).
43. Liu, L. & Ji, S. A new contact detection method for arbitrary dilated polyhedra with potential function in discrete element method. *Int. J. Numer. Methods Eng.* **121**, 5742–5765 (2020).
44. Shao, L., Mao, J., Zhao, L. & Li, T. A three-dimensional deformable spheropolyhedral-based discrete element method for simulation of the whole fracture process. *Eng. Fract. Mech.* **263**, 108290 (2022).
45. Delaney, G. W. & Cleary, P. W. The packing properties of superellipsoids. *Europhys. Lett.* **89**, 34002 (2010).
46. Wellmann, C., Lillie, C. & Wriggers, P. A contact detection algorithm for superellipsoids based on the common-normal concept. *Eng. Comput.* **25**, 432–442 (2008).
47. Zhao, S., Zhang, N., Zhou, X. & Zhang, L. Particle shape effects on fabric of granular random packing. *Powder Technol.* **310**, 175–186 (2017).
48. Peters, J. F., Hopkins, M. A., Kala, R. & Wahl, R. E. A poly-ellipsoid particle for non-spherical discrete element method. *Eng. Comput.* **26**, 645–657 (2009).
49. Zhang, B., Regueiro, R., Druckrey, A. & Alshibli, K. Construction of poly-ellipsoidal grain shapes from SMT imaging on sand, and the development of a new DEM contact detection algorithm. *Eng. Comput.* **35**, 733–771 (2018).

50. Zhao, S. & Zhao, J. A poly-superellipsoid-based approach on particle morphology for DEM modeling of granular media. *Int. J. Numer. Anal. Methods Geomech.* **43**, 2147–2169 (2019).
51. Lai, Z. & Huang, L. A polybézier-based particle model for the DEM modeling of granular media. *Comput. Geotech.* **134**, 104052 (2021).
52. Zhang, P., Dong, Y., Galindo-Torres, S. A., Scheuermann, A. & Li, L. Metaball based discrete element method for general shaped particles with round features. *Comput. Mech.* **67**, 1243–1254 (2021).
53. Craveiro, M. V., Neto, A. G. & Wriggers, P. Contact between rigid convex NURBS particles based on computer graphics concepts. *Comput. Methods Appl. Mech. Eng.* **386**, 114097 (2021).
54. Lim, K.-W., Krabbenhoft, K. & Andrade, J. E. On the contact treatment of non-convex particles in the granular element method. *Comp. Part. Mech.* **1**, 257–275 (2014).
55. Mollon, G. & Zhao, J. 3D generation of realistic granular samples based on random fields theory and Fourier shape descriptors. *Comput. Methods Appl. Mech. Eng.* **279**, 46–65 (2014).
56. Zhou, B. & Wang, J. Generation of a realistic 3D sand assembly using X-ray micro-computed tomography and spherical harmonic-based principal component analysis: generation of a realistic 3D sand assembly. *Int. J. Numer. Anal. Meth. Geomech.* **41**, 93–109 (2017).
57. Sun, Q. & Zheng, J. Clone granular soils with mixed particle morphological characteristics by integrating spherical harmonics with Gaussian mixture model, expectation-maximization, and Dirichlet process. *Acta Geotech.* **15**, 2779–2796 (2020).
58. Bardhan, J. P. & Knepley, M. G. Computational science and re-discovery: open-source implementation of ellipsoidal harmonics for problems in potential theory. *Comput. Sci. Disc.* **5**, 014006 (2012).
59. Klotz, T. S., Bardhan, J. P. & Knepley, M. G. Efficient evaluation of ellipsoidal harmonics for potential modeling. Preprint at *arXiv* https://doi.org/10.48550/arXiv.1708.06028 (2017).
60. Reimond, S. & Baur, O. Spheroidal and ellipsoidal harmonic expansions of the gravitational potential of small Solar System bodies. Case study: comet 67P/Churyumov-Gerasimenko: gravitational potential of small bodies. *J. Geophys. Res. Planets* **121**, 497–515 (2016).
61. Cundall, P. A. & Strack, O. D. L. A discrete numerical model for granular assemblies. *Géotechnique* **29**, 47–65 (1979).
62. Smallenburg, F. Efficient event-driven simulations of hard spheres. *Eur. Phys. J. E* **45**, 22 (2022).
63. Cantor, D., Azema, E. & Preechawuttipong, I. Microstructural analysis of sheared polydisperse polyhedral grains. *Phys. Rev. E* **101**, 062901 (2020).
64. Wachs, A. Particle-scale computational approaches to model dry and saturated granular flows of non-Brownian, non-cohesive, and non-spherical rigid bodies. *Acta Mech.* **230**, 1919–1980 (2019).
65. Radjai, F. & Richefeu, V. Contact dynamics as a nonsmooth discrete element method. *Mech. Mater.* **41**, 715–728 (2009).
66. Dubois, F., Acary, V. & Jean, M. The contact dynamics method: a nonsmooth story. *C. R. Méc.* **346**, 247–262 (2018).
67. Hahn, J. K. Realistic animation of rigid bodies. *SIGGRAPH Comput. Graph.* **22**, 299–308 (1988).
68. Tang, X., Paluszny, A. & Zimmerman, R. W. An impulse-based energy tracking method for collision resolution. *Comput. Methods Appl. Mech. Eng.* **278**, 160–185 (2014).
69. Lee, S. J. & Hashash, Y. M. A. iDEM: an impulse-based discrete element method for fast granular dynamics. *Int. J. Numer. Methods Eng.* **104**, 79–103 (2015).
70. Jehser, M. & Likos, C. N. Aggregation shapes of amphiphilic ring polymers: from spherical to toroidal micelles. *Colloid Polym. Sci.* **298**, 735–745 (2020).
71. Donev, A., Torquato, S. & Stillinger, F. H. Neighbor list collision-driven molecular dynamics simulation for nonspherical hard particles. II. Applications to ellipses and ellipsoids. *J. Comput. Phys.* **202**, 765–793 (2005).
72. Skora, T., Vaghefikia, F., Fitter, J. & Kondrat, S. Macromolecular crowding: how shape and interactions affect diffusion. *J. Phys. Chem. B* **124**, 7537–7543 (2020).
73. Baldauf, L., Teich, E. G., Schall, P., van Anders, G. & Rossi, L. Shape and interaction decoupling for colloidal preassembly. *Sci. Adv.* **8**, eabm0548 (2022).
74. Chiappini, M. & Dijkstra, M. A generalized density-modulated twist-splay-bend phase of banana-shaped particles. *Nat. Commun.* **12**, 2157 (2021).
75. Pal, A. et al. Shape matters in magnetic-field-assisted assembly of prolate colloids. *ACS Nano* **16**, 2558–2568 (2022).
76. Ferrari, F., Lavagna, M. & Blazquez, E. A parallel-GPU code for asteroid aggregation problems with angular particles. *Mon. Not. Roy. Astron. Soc.* **492**, 749–761 (2020).
77. Zhao, S., Lai, Z. & Zhao, J. Leveraging ray tracing cores for particle-based simulations on GPUs. *Int. J. Numer. Methods Eng.* **124**, 696–713 (2022).
78. Howard, M. P., Anderson, J. A., Nikoubashman, A., Glotzer, S. C. & Panagiotopoulos, A. Z. Efficient neighbor list calculation for molecular simulation of colloidal systems using graphics processing units. *Comput. Phys. Commun.* **203**, 45–52 (2016).
79. Donev, A., Torquato, S. & Stillinger, F. H. Neighbor list collision-driven molecular dynamics simulation for nonspherical hard particles. I. Algorithmic details. *J. Comput. Phys.* **202**, 737–764 (2005).
80. Girault, I., Chadil, M.-A. & Vincent, S. Comparison of methods computing the distance between two ellipsoids. *J. Comput. Phys.* **458**, 111100 (2022).
81. Eliáš, J. Simulation of railway ballast using crushable polyhedral particles. *Powder Technol.* **264**, 458–465 (2014).
82. Zhao, S., Zhou, X. & Liu, W. Discrete element simulations of direct shear tests with particle angularity effect. *Granul. Matter* **17**, 793–806 (2015).
83. Günther, O. & Wong, E. A dual approach to detect polyhedral intersections in arbitrary dimensions. *BIT Numer. Math.* **31**, 2–14 (1991).
84. Feng, Y. T. An effective energy-conserving contact modelling strategy for spherical harmonic particles represented by surface triangular meshes with automatic simplification. *Comput. Methods Appl. Mech. Eng.* **379**, 113750 (2021).
85. Lai, Z., Chen, Q. & Huang, L. Fourier series-based discrete element method for computational mechanics of irregular-shaped particles. *Comput. Methods Appl. Mech. Eng.* **362**, 112873 (2020).
86. He, H. & Zheng, J. Simulations of realistic granular soils in oedometer tests using physics engine. *Int. J. Numer. Anal. Methods Geomech.* **44**, 983–1002 (2020).
87. Zhu, F. & Zhao, J. Modeling continuous grain crushing in granular media: a hybrid peridynamics and physics engine approach. *Comput. Methods Appl. Mech. Eng.* **348**, 334–355 (2019).
88. Ramasubramani, V., Vo, T., Anderson, J. A. & Glotzer, S. C. A mean-field approach to simulating anisotropic particles. *J. Chem. Phys.* **153**, 084106 (2020).
89. Lubachevsky, B. D. & Stillinger, F. H. Geometric properties of random disk packings. *J. Stat. Phys.* **60**, 561–583 (1990).
90. Maher, C. E., Stillinger, F. H. & Torquato, S. Characterization of void space, large-scale structure, and transport properties of maximally random jammed packings of superballs. *Phys. Rev. Mater.* **6**, 025603 (2022).
91. Cundall, P. A. Formulation of a three-dimensional distinct element model — part I. A scheme to detect and represent contacts in a system composed of many polyhedral blocks. *Int. J. Rock Mech. Min. Sci. Geomech. Abstr.* **25**, 107–116 (1988).
92. Nezami, E. G., Hashash, Y. M. A., Zhao, D. W. & Ghaboussi, J. A fast contact detection algorithm for 3-D discrete element method. *Comput. Geotech.* **31**, 575–587 (2004).
93. Azéma, E., Radjai, F. & Dubois, F. Packings of irregular polyhedral particles: strength, structure, and effects of angularity. *Phys. Rev. E* **87**, 062203 (2013).
94. Zhan, L., Peng, C., Zhang, B. & Wu, W. A surface mesh represented discrete element method (SMR-DEM) for particles of arbitrary shape. *Powder Technol.* **377**, 760–779 (2021).
95. Capozza, R. & Hanley, K. J. A hierarchical, spherical harmonic-based approach to simulate abradable, irregularly shaped particles in DEM. *Powder Technol.* **378**, 528–537 (2021).
96. Wang, X., Yin, Z.-Y., Xiong, H., Su, D. & Feng, Y.-T. A spherical-harmonic-based approach to discrete element modeling of 3D irregular particles. *Int. J. Numer. Methods Eng.* **122**, 5626–5655 (2021).
97. Kawamoto, R., Andò, E., Viggiani, G. & Andrade, J. E. Level set discrete element method for three-dimensional computations with triaxial case study. *J. Mech. Phys. Solids* **91**, 1–13 (2016).
98. Harmon, J. M., Arthur, D. & Andrade, J. E. Level set splitting in DEM for modeling breakage mechanics. *Comput. Methods Appl. Mech. Eng.* **365**, 112961 (2020).
99. Duriez, J. & Galusinski, C. A level set-discrete element method in YADE for numerical, micro-scale, geomechanics with refined grain shapes. *Comput. Geosci.* **157**, 104936 (2021).
100. Lai, Z., Zhao, S., Zhao, J. & Huang, L. Signed distance field framework for unified DEM modeling of granular media with arbitrary particle shapes. *Comput. Mech.* **70**, 763–783 (2022).
101. Mori, Y. & Sakai, M. Advanced DEM simulation on powder mixing for ellipsoidal particles in an industrial mixer. *Chem. Eng. J.* **429**, 132415 (2022).
102. Huang, S., Huang, L., Lai, Z. & Zhao, J. Morphology characterization and discrete element modeling of coral sand with intraparticle voids. *Eng. Geol.* **315**, 107023 (2023).
103. Feng, Y. T. An energy-conserving contact theory for discrete element modelling of arbitrarily shaped particles: basic framework and general contact model. *Comput. Methods Appl. Mech. Eng.* **373**, 113454 (2021).
104. Hoque, S. Z., Anand, D. V. & Patnaik, B. S. A dissipative particle dynamics simulation of a pair of red blood cells in flow through a symmetric and an asymmetric bifurcated microchannel. *Comput. Part. Mech.* **9**, 1219–1231 (2022).
105. Villone, M. M. & Maffettone, P. L. Dynamics, rheology, and applications of elastic deformable particle suspensions: a review. *Rheol. Acta* **58**, 109–130 (2019).
106. Norouzi, M., Andric, J., Vernet, A. & Pallares, J. Shape evolution of long flexible fibers in viscous flows. *Acta Mech.* **233**, 2077–2091 (2022).
107. Emiroglu, D. B. et al. Building block properties govern granular hydrogel mechanics through contact deformations. *Sci. Adv.* **8**, eadd8570 (2022).
108. Tavares, L. M. & das Chagas, A. S. A stochastic particle replacement strategy for simulating breakage in DEM. *Powder Technol.* **377**, 222–232 (2021).
109. Jiang, Y., Mora, P., Herrmann, H. J. & Alonso-Marroquín, F. Damage separation model: a replaceable particle method based on strain energy field. *Phys. Rev. E* **104**, 045311 (2021).
110. Orozco, L. F., Delenne, J.-Y., Sornay, P. & Radjai, F. Scaling behavior of particle breakage in granular flows inside rotating drums. *Phys. Rev. E* **101**, 052904 (2020).
111. Ramkrishna, D. & Singh, M. R. Population balance modeling: current status and future prospects. *Annu. Rev. Chem. Biomol. Eng.* **5**, 123–146 (2014).
112. Cabiscol, R., Finke, J. H. & Kwade, A. A bi-directional DEM-PBM coupling to evaluate chipping and abrasion of pharmaceutical tablets. *Adv. Powder Technol.* **32**, 2839–2855 (2021).
113. Kuang, D.-M., Long, Z.-L., Ogwu, I. & Chen, Z. A discrete element method (DEM)-based approach to simulating particle breakage. *Acta Geotech.* **17**, 2751–2764 (2022).

114. Fang, C., Gong, J., Nie, Z., Li, B. & Li, X. DEM study on the microscale and macroscale shear behaviours of granular materials with breakable and irregularly shaped particles. *Comput. Geotech.* **137**, 104271 (2021).
115. Nguyen, D.-H., Azéma, E., Sornay, P. & Radjai, F. Bonded-cell model for particle fracture. *Phys. Rev. E* **91**, 022203 (2015).
116. Cantor, D., Azéma, E., Sornay, P. & Radjai, F. Three-dimensional bonded-cell model for grain fragmentation. *Comp. Part. Mech.* **4**, 441–450 (2017).
117. Nikolić, M., Karavelić, E., Ibrahimbegovic, A. & Miščević, P. Lattice element models and their peculiarities. *Arch. Comput. Methods Eng.* **25**, 753–784 (2018).
118. Delenne, J.-Y., Topin, V. & Radjai, F. Failure of cemented granular materials under simple compression: experiments and numerical simulations. *Acta Mech.* **205**, 9–21 (2009).
119. Affes, R., Delenne, J.-Y., Monerie, Y., Radjaï, F. & Topin, V. Tensile strength and fracture of cemented granular aggregates. *Eur. Phys. J. E* **35**, 117 (2012).
120. Topin, V., Radjaï, F., Delenne, J.-Y. & Mabille, F. Mechanical modeling of wheat hardness and fragmentation. *Powder Technol.* **190**, 215–220 (2009).
121. Sargado, J. M., Keilegavlen, E., Berre, I. & Nordbotten, J. M. A combined finite element–finite volume framework for phase-field fracture. *Comput. Methods Appl. Mech. Eng.* **373**, 113474 (2021).
122. Rahimi, M. N. & Moutsanidis, G. A smoothed particle hydrodynamics approach for phase field modeling of brittle fracture. *Comput. Methods Appl. Mech. Eng.* **398**, 115191 (2022).
123. Mohajerani, S. & Wang, G. 'Touch-aware' contact model for peridynamics modeling of granular systems. *Int. J. Numer. Methods Eng.* **123**, 3850–3878 (2022).
124. Zhu, F. & Zhao, J. Multiscale modeling of continuous crushing of granular media: the role of grain microstructure. *Comput. Part. Mech.* **8**, 1089–1101 (2021).
125. Pezeshkian, W. & Marrink, S. J. Simulating realistic membrane shapes. *Curr. Opin. Cell Biol.* **71**, 103–111 (2021).
126. Li, B. & Abel, S. M. Membrane-mediated interactions between hinge-like particles. *Soft Matter* **18**, 2742–2749 (2022).
127. Boromand, A. et al. The role of deformability in determining the structural and mechanical properties of bubbles and emulsions. *Soft Matter* **15**, 5854–5865 (2019).
128. Treado, J. D. et al. Bridging particle deformability and collective response in soft solids. *Phys. Rev. Mater.* **5**, 055605 (2021).
129. Tran, S. B. Q., Le, Q. T., Leong, F. Y. & Le, D. V. Modeling deformable capsules in viscous flow using immersed boundary method. *Phys. Fluids* **32**, 093602 (2020).
130. Gay Neto, A., Hudobivnik, B., Moherdaui, T. F. & Wriggers, P. Flexible polyhedra modeled by the virtual element method in a discrete element context. *Comput. Methods Appl. Mech. Eng.* **387**, 114163 (2021).
131. Rahmati, S., Zuniga, A., Jodoin, B. & Veiga, R. G. A. Deformation of copper particles upon impact: a molecular dynamics study of cold spray. *Comput. Mater. Sci.* **171**, 109219 (2020).
132. Liu, X. et al. Discrete element-embedded finite element model for simulation of soft particle motion and deformation. *Particuology* **68**, 88–100 (2022).
133. Cardenas-Barrantes, M., Cantor, D., Bares, J., Renouf, M. & Azema, E. Micromechanical description of the compaction of soft pentagon assemblies. *Phys. Rev. E* **103**, 062902 (2021).
134. Nezamabadi, S., Radjai, F., Averseng, J. & Delenne, J.-Y. Implicit frictional-contact model for soft particle systems. *J. Mech. Phys. Solids* **83**, 72–87 (2015).
135. Nezamabadi, S., Ghadiri, M., Delenne, J.-Y. & Radjai, F. Modelling the compaction of plastic particle packings. *Comput. Part. Mech.* **9**, 45–52 (2022).
136. Brunk, N. E., Kadupitiya, J. C. S. & Jadhao, V. Designing surface charge patterns for shape control of deformable nanoparticles. *Phys. Rev. Lett.* **125**, 248001 (2020).
137. Harting, J. et al. Recent advances in the simulation of particle-laden flows. *Eur. Phys. J. Spec. Top.* **223**, 2253–2267 (2014).
138. Robinson, M., Luding, S. & Ramaioli, M. Fluid-particle flow and validation using two-way-coupled mesoscale SPH-DEM. *Int. J. Multiph. Flow* **59**, 121–134 (2014).
139. Vowinckel, B. Incorporating grain-scale processes in macroscopic sediment transport models: a review and perspectives for environmental and geophysical applications. *Acta Mech.* **232**, 2023–2050 (2021).
140. Zhang, X. & Tahmasebi, P. Coupling irregular particles and fluid: complex dynamics of granular flows. *Comput. Geotech.* **143**, 104624 (2022).
141. Shrestha, S., Kuang, S. B., Yu, A. B. & Zhou, Z. Y. Effect of van der Waals force on bubble dynamics in bubbling fluidized beds of ellipsoidal particles. *Chem. Eng. Sci.* **212**, 115343 (2020).
142. Jain, R., Tschisgale, S. & Froehlich, J. Effect of particle shape on bedload sediment transport in case of small particle loading. *Meccanica* **55**, 299–315 (2020).
143. Shaebani, M. R., Wysocki, A., Winkler, R. G., Gompper, G. & Rieger, H. Computational models for active matter. *Nat. Rev. Phys.* **2**, 181–199 (2020).
144. Aliu, O., Sakidin, H., Foroozesh, J. & Yahya, N. Lattice Boltzmann application to nanofluids dynamics — a review. *J. Mol. Liq.* **300**, 112284 (2020).
145. de Graaf, J. et al. Lattice-Boltzmann hydrodynamics of anisotropic active matter. *J. Chem. Phys.* **144**, 134106 (2016).
146. Lee, M., Lohrmann, C., Szuttor, K., Auradou, H. & Holm, C. The influence of motility on bacterial accumulation in a microporous channel. *Soft Matter* **17**, 893–902 (2021).
147. Yang, Q. et al. Capillary condensation under atomic-scale confinement. *Nature* **588**, 250–253 (2020).
148. Yang, L., Sega, M. & Harting, J. Capillary-bridge forces between solid particles: insights from lattice Boltzmann simulations. *AIChE J.* **67**, e17350 (2021).
149. Delenne, J.-Y., Richefeu, V. & Radjai, F. Liquid clustering and capillary pressure in granular media. *J. Fluid Mech.* **762**, R5 (2015).
150. Wang, S., Wu, Q. & He, Y. Estimation of the fluidization behavior of nonspherical wet particles with liquid transfer. *Ind. Eng. Chem. Res.* **61**, 10254–10263 (2022).
151. Mittal, K., Dutta, S. & Fischer, P. Direct numerical simulation of rotating ellipsoidal particles using moving nonconforming Schwarz-spectral element method. *Comput. Fluids* **205**, 104556 (2020).
152. Reder, M., Hoffrogge, P. W., Schneider, D. & Nestler, B. A phase-field based model for coupling two-phase flow with the motion of immersed rigid bodies. *Int. J. Numer. Methods Eng.* **123**, 3757–3780 (2022).
153. Jabeen, S., Usman, K. & Shahid, M. Numerical study of general shape particles in a concentric annular duct having inner obstacle. *Comput. Part. Mech.* **9**, 485–497 (2022).
154. Peskin, C. S. The immersed boundary method. *Acta Numer.* **11**, 479–517 (2002).
155. Wu, M., Peters, B., Rosemann, T. & Kruggel-Emden, H. A forcing fictitious domain method to simulate fluid–particle interaction of particles with super-quadric shape. *Powder Technol.* **360**, 264–277 (2020).
156. Isoz, M., Sourek, M. K., Studenik, O. & Koci, P. Hybrid fictitious domain-immersed boundary solver coupled with discrete element method for simulations of flows laden with arbitrarily-shaped particles. *Comput. Fluids* **244**, 105538 (2022).
157. Uhlmann, M. An immersed boundary method with direct forcing for the simulation of particulate flows. *J. Comput. Phys.* **209**, 448–476 (2005).
158. Lauber, M., Weymouth, G. D. & Limbert, G. Immersed boundary simulations of flows driven by moving thin membranes. *J. Comput. Phys.* **457**, 111076 (2022).
159. Yamamoto, R., Molina, J. J. & Nakayama, Y. Smoothed profile method for direct numerical simulations of hydrodynamically interacting particles. *Soft Matter* **17**, 4226–4253 (2021).
160. Aniello, A. et al. Comparison of a finite volume and two lattice Boltzmann solvers for swirled confined flows. *Comput. Fluids* **241**, 105463 (2022).
161. Patel, K. & Stark, H. A pair of particles in inertial microfluidics: effect of shape, softness, and position. *Soft Matter* **17**, 4804–4817 (2021).
162. Cheng, H., Luding, S., Rivas, N., Harting, J. & Magnanimo, V. Hydro-micromechanical modeling of wave propagation in saturated granular crystals. *Int. J. Numer. Anal. Methods Geomech.* **43**, 1115–1139 (2019).
163. Lind, S. J., Rogers, B. D. & Stansby, P. K. Review of smoothed particle hydrodynamics: towards converged Lagrangian flow modelling. *Proc. R. Soc. A Math. Phys. Eng. Sci.* **476**, 20190801 (2020).
164. Canelas, R. B., Crespo, A. J. C., Domínguez, J. M., Ferreira, R. M. L. & Gómez-Gesteira, M. SPH–DCDEM model for arbitrary geometries in free surface solid–fluid flows. *Comput. Phys. Commun.* **202**, 131–140 (2016).
165. Bouscasse, B., Colagrossi, A., Marrone, S. & Antuono, M. Nonlinear water wave interaction with floating bodies in SPH. *J. Fluids Struct.* **42**, 112–129 (2013).
166. Trujillo-Vela, M. G., Galindo-Torres, S. A., Zhang, X., Ramos-Cañón, A. M. & Escobar-Vargas, J. A. Smooth particle hydrodynamics and discrete element method coupling scheme for the simulation of debris flows. *Comput. Geotech.* **125**, 103669 (2020).
167. Peng, C., Zhan, L., Wu, W. & Zhang, B. A fully resolved SPH-DEM method for heterogeneous suspensions with arbitrary particle shape. *Powder Technol.* **387**, 509–526 (2021).
168. Chen, H., Zhao, S., Zhao, J. & Zhou, X. DEM-enriched contact approach for material point method. *Comput. Methods Appl. Mech. Eng.* **404**, 115814 (2023).
169. Español, P. & Warren, P. B. Perspective: dissipative particle dynamics. *J. Chem. Phys.* **146**, 150901 (2017).
170. Zhang, J. & Choi, C. E. Improved settling velocity for microplastic fibers: a new shape-dependent drag model. *Environ. Sci. Technol.* **56**, 962–973 (2022).
171. Zhong, W., Yu, A., Liu, X., Tong, Z. & Zhang, H. DEM/CFD-DEM modelling of non-spherical particulate systems: theoretical developments and applications. *Powder Technol.* **302**, 108–152 (2016).
172. Yang, F., Zeng, Y.-H. & Huai, W.-X. A new model for settling velocity of non-spherical particles. *Environ. Sci. Pollut. Res.* **28**, 61636–61646 (2021).
173. Castang, C., Lain, S., Garcia, D. & Sommerfeld, M. Aerodynamic coefficients of irregular non-spherical particles at intermediate Reynolds numbers. *Powder Technol.* **402**, 117341 (2022).
174. Livi, C., Di Staso, G., Clercx, H. J. H. & Toschi, F. Drag and lift coefficients of ellipsoidal particles under rarefied flow conditions. *Phys. Rev. E* **105**, 015306 (2022).
175. Chen, S., Chen, P. & Fu, J. Drag and lift forces acting on linear and irregular agglomerates formed by spherical particles. *Phys. Fluids* **34**, 023307 (2022).
176. Tagliavini, G. et al. Drag coefficient prediction of complex-shaped snow particles falling in air beyond the Stokes regime. *Int. J. Multiph. Flow* **140**, 103652 (2021).
177. Dey, S., Ali, S. Z. & Padhi, E. Terminal fall velocity: the legacy of Stokes from the perspective of fluvial hydraulics. *Proc. R. Soc. A Math. Phys. Eng. Sci.* **475**, 20190277 (2019).
178. Bonazzi, F., Hall, C. K. & Weikl, T. R. Membrane morphologies induced by mixtures of arc-shaped particles with opposite curvature. *Soft Matter* **17**, 268–275 (2021).
179. Cheng, H., Thornton, A. R., Luding, S., Hazel, A. L. & Weinhart, T. Concurrent multi-scale modeling of granular materials: role of coarse-graining in FEM–DEM coupling. *Comput. Methods Appl. Mech. Eng.* **403**, 115651 (2023).
180. Xu, X., Li, C. & Gao, X. Coarse-grained DEM-CFD simulation of fluidization behavior of irregular shape sand particles. *Ind. Eng. Chem. Res.* **61**, 9099–9109 (2022).
181. Yue, Y. et al. Hybrid grains: adaptive coupling of discrete and continuum simulations of granular media. in *SIGGRAPH Asia 2018 Technical Papers on — SIGGRAPH Asia '18* 1–19 (ACM Press, 2018). https://doi.org/10.1145/3272127.3275095.
182. Guo, N. & Zhao, J. Parallel hierarchical multiscale modelling of hydro-mechanical problems for saturated granular soils. *Comput. Methods Appl. Mech. Eng.* **305**, 37–61 (2016).

183. Zhao, S., Zhao, J. & Lai, Y. Multiscale modeling of thermo-mechanical responses of granular materials: a hierarchical continuum–discrete coupling approach. *Comput. Methods Appl. Mech. Eng.* **367**, 113100 (2020).
184. Liang, W. & Zhao, J. Multiscale modeling of large deformation in geomechanics. *Int. J. Numer. Anal. Methods Geomech.* **43**, 1080–1114 (2019).
185. Zhao, S., Zhao, J., Liang, W. & Niu, F. Multiscale modeling of coupled thermo-mechanical behavior of granular media in large deformation and flow. *Comput. Geotech.* **149**, 104855 (2022).
186. Jaeggi, A., Rajagopalan, A. K., Morari, M. & Mazzotti, M. Characterizing ensembles of platelike particles via machine learning. *Ind. Eng. Chem. Res.* **60**, 473–483 (2021).
187. Zhang, H. et al. Characterization of particle size and shape by an IPI system through deep learning. *J. Quant. Spectrosc. Radiat. Transf.* **268**, 107642 (2021).
188. Hwang, S., Pan, J., Sunny, A. A. & Fan, L.-S. A machine learning-based particle–particle collision model for non-spherical particles with arbitrary shape. *Chem. Eng. Sci.* **251**, 117439 (2022).
189. Lai, Z., Chen, Q. & Huang, L. Machine-learning-enabled discrete element method: contact detection and resolution of irregular-shaped particles. *Int. J. Numer. Anal. Methods Geomech.* **46**, 113–140 (2022).
190. Yan, S.-N., Wang, T.-Y., Tang, T.-Q., Ren, A.-X. & He, Y.-R. Simulation on hydrodynamics of non-spherical particulate system using a drag coefficient correlation based on artificial neural network. *Pet. Sci.* **17**, 537–555 (2020).
191. Hwang, S., Pan, J. & Fan, L.-S. A machine learning-based interaction force model for non-spherical and irregular particles in low Reynolds number incompressible flows. *Powder Technol.* **392**, 632–638 (2021).
192. Cheng, H. et al. An iterative Bayesian filtering framework for fast and automated calibration of DEM models. *Comput. Methods Appl. Mech. Eng.* **350**, 268–294 (2019).
193. Ma, G., Guan, S., Wang, Q., Feng, Y. T. & Zhou, W. A predictive deep learning framework for path-dependent mechanical behavior of granular materials. *Acta Geotech.* **17**, 3463–3478 (2022).
194. Wang, K. et al. A physics-informed and hierarchically regularized data-driven model for predicting fluid flow through porous media. *J. Comput. Phys.* **443**, 110526 (2021).
195. Karniadakis, G. E. et al. Physics-informed machine learning. *Nat. Rev. Phys.* **3**, 422–440 (2021).
196. Park, E. H., Kindratenko, V. & Hashash, Y. M. A. Shared memory parallelization for high-fidelity large-scale 3D polyhedral particle simulations. *Comput. Geotech.* **137**, 104008 (2021).
197. Gao, X., Yu, J., Lu, L., Li, C. & Rogers, W. A. Development and validation of SuperDEM–CFD coupled model for simulating non-spherical particles hydrodynamics in fluidized beds. *Chem. Eng. J.* **420**, 127654 (2021).
198. Wu, C. et al. System-level modeling of GPU/FPGA clusters for molecular dynamics simulations. in *2021 IEEE High Performance Extreme Computing Conference (HPEC)* 1–8 (IEEE, 2021). https://doi.org/10.1109/HPEC49654.2021.9622838.
199. Weinhart, T., Fuchs, R., Staedler, T., Kappl, M. & Luding, S. Sintering — pressure- and temperature-dependent contact models. in *Particles in Contact* (ed. Antonyuk, S.) 311–338 (Springer International Publishing, 2019). https://doi.org/10.1007/978-3-030-15899-6_10.
200. Taghizadeh, K., Steeb, H., Luding, S. & Magnanimo, V. Elastic waves in particulate glass–rubber mixtures. *Proc. R. Soc. A Math. Phys. Eng. Sci.* **477**, 20200834 (2021).
201. Luding, S. Introduction to discrete element methods. *Eur. J. Environ. Civ. Eng.* **12**, 785–826 (2008).
202. Angelidakis, V., Nadimi, S., Otsubo, M. & Utili, S. CLUMP: a code library to generate universal multi-sphere particles. *SoftwareX* **15**, 100735 (2021).
203. Ferellec, J. & McDOWELL, G. Modelling realistic shape and particle inertia in DEM. *Géotechnique* **60**, 227–232 (2010).
204. Zhao, S., Chen, H. & Zhao, J. Multiscale modeling of freeze–thaw behavior in granular media. *Acta Mech. Sin.* **39**, 722195 (2023).
205. Zhao, S. & Zhao, J. SudoDEM: unleashing the predictive power of the discrete element method on simulation for non-spherical granular particles. *Comput. Phys. Commun.* **259**, 107670 (2021).
206. Ye, T., Phan-Thien, N. & Lim, C. T. Particle-based simulations of red blood cells — a review. *J. Biomech.* **49**, 2255–2266 (2016).
207. Nagata, T. et al. A simple collision algorithm for arbitrarily shaped objects in particle-resolved flow simulation using an immersed boundary method. *Int. J. Numer. Methods Fluids* **92**, 1256–1273 (2020).

Acknowledgements

J.Z. and S.Z. acknowledge the financial supports from the National Natural Science Foundation of China (via Project Nos 11972030 and 51909095) and Research Grants Council of Hong Kong (GRF Projects Nos 16206322, 16208720 and 16211221 and F-HKUST601/19). J.Z. also acknowledges the supports by the Project of Hetao Shenzhen-Hong Kong Science and Technology Innovation Cooperation Zone (HZQB-KCZYB-2020083) and the internal research supports provided by HKUST (FP907, IEG22EG01 and IEG22EG01PG).

Author contributions

All authors contributed to all aspects of manuscript preparation, revision and editing.

Competing interests

The authors declare no competing interests.

Additional information

Peer review information *Nature Reviews Physics* thanks Devang Khakhar, Farhang Radjai and the other, anonymous, reviewer(s) for their contribution to the peer review of this work.